

Selective targeting of the anti-viral drug lamivudine to the liver

by

Krishna Chaitanya Chimalakonda, B.Pharm.

A THESIS

IN

PHARMACEUTICAL SCIENCES

Submitted to the Graduate Faculty of
Texas Tech University Health Sciences Center
in Partial Fulfillment of the Requirements
for the Degree of

MASTER OF SCIENCE

Advisory Committee

Reza Mehvar (Chairperson)
Ulrich Bickel
Jochen Klein

Accepted

Arthur Nelson
Dean of the Graduate School of Biomedical Sciences
Texas Tech University Health Sciences Center

August 2007

ACKNOWLEDGMENTS

I greatly thank my advisor Dr Reza Mehvar, Pharm. D., Ph.D. for all his help, time, patience, guidance, care, and support. This dissertation would not have been possible without his advice, inspiration, and motivation. I feel greatly indebted to Dr. Mehvar for providing me with an opportunity to work under his able guidance.

I also thank my M.S. Advisory committee members Ulrich Bickel, M.D. and Jochen Klein, Ph.D. for their valuable suggestions.

I am ever thankful to my parents, brother, and friends for their continuous love, care, and affection.

TABLE OF CONTENTS

Acknowledgments.....	ii
Abstract.....	v
List of Tables.....	vii
List of Figures.....	viii
Chapter	
1. Introduction.....	1
1.1. Goals of antiviral therapy.....	2
1.2. Agents for the treatment of chronic hepatitis B.....	3
1.3. Lamivudine.....	4
1.3.1. Pharmacokinetics.....	7
1.3.1.1. Absorption.....	7
1.3.1.2. Effect of food on absorption.....	8
1.3.1.3. Distribution.....	8
1.3.1.4. Metabolism and elimination.....	9
1.3.1.5. Effect of hepatic dysfunction.....	10
1.3.1.6. Effects of renal dysfunction.....	11
1.3.1.7. Multiple dose pharmacokinetics.....	11
1.3.1.8. Drug interactions.....	12
1.3.2. Adverse effects.....	12
1.3.3. Dosage and administration.....	14
1.3.4. Place of lamivudine in the management of chronic hepatitis B.....	14
1.4. Drug delivery approaches in Hepatitis B treatment.....	16
1.4.1. Macromolecular prodrug approaches.....	16
1.4.1.1. Protein and glycoprotein carriers.....	16
1.4.1.2. Poly L-lysine carriers.....	19
1.4.1.3. Polysaccharide carriers.....	21
1.4.1.3.1. Arabinogalactan.....	21
1.4.1.3.2. Dextrans.....	22
1.4.2. Other approaches.....	22
1.5. Dextrans as macromolecular carriers.....	23
1.5.1. Physicochemical properties.....	24
1.5.2. Lack of oral availability of dextrans.....	25
1.5.3. Plasma kinetics.....	25
1.5.4. Renal clearance.....	26
1.5.5. Metabolism.....	27
1.5.6. Molecular-weight-and dose-dependent tissue distribution and accumulation..	28
1.5.7. Effect of electrical charge on the kinetics of dextrans.....	29
1.5.8. Kinetics of dextrans modified for receptor-mediated targeting.....	30
1.6. Hypothesis and specific Aims.....	32
2. Materials and Methods.....	34
2.1. Chemicals.....	34
2.2. Animals.....	34
2.3. Synthesis of 3TC-succinate-dextran (3TCSD) conjugate.....	34

2.3.1. (-)-5'-O-(tert-Butyldimethylsilyloxy)-2',3'-dideoxy-3'-thiacytidine (2).....	35
2.3.2. (-)-4-N-(4,4'-Dimethoxytrityl)-5'-O-(tert-butyldimethylsilyloxy)-2',3'-dideoxy-3'-thia-cytidine (3).....	36
2.3.3. (-)-4-N-(4,4'-Dimethoxytrityl)-2',3'-dideoxy-3'-thiacytidine (4)	36
2.3.4. (-)-4-N-(4,4'-Dimethoxytrityl)-5'-O-(succinate)-2',3'-dideoxy-3'-thiacytidine (5) .	37
2.3.5. (-)-5'-O-(Succinate)-2',3'-dideoxy-3'-thiacytidine (3TCS, 6)	38
2.3.6. (-)-Dextran-5'-O-(succinate)-2',3'-dideoxy-3'-thiacytidine (3TC-succinate-dextran conjugate, 3TCSD, 8)	38
2.4. Further characterization of 3TC-succinate-dextran conjugate (3TCSD, 8).....	39
2.5. High performance liquid chromatography.....	40
2.5.1. Size-exclusion liquid chromatography (SEC)	40
2.5.2. Reversed-phase liquid chromatography (RPC)	40
2.5.3. HPLC system	41
2.5.4. Standard solutions.....	41
2.5.5. Sample preparation	41
2.5.6. Validation of assays	43
2.5.7. Recovery	43
2.6. In vitro release characteristic	43
2.6.1. Release characteristics in buffers.....	43
2.6.2. Release characteristics in rat blood.....	44
2.6.3. Release characteristics in rat liver lysosomes.....	44
2.7. In vivo disposition.....	45
2.8. Pharmacokinetic analysis.....	46
2.9. Statistical analysis.....	47
3. Results.....	48
3.1. Synthesis and characterization of 3TCSD	48
3.2. Size-exclusion chromatographic method.....	51
3.3. Reversed-phase chromatographic method.....	54
3.4. Release characteristics in buffers.....	57
3.5. Release characteristics in rat blood.....	60
3.6. Release characteristics in rat liver lysosomes.....	62
3.7. In vivo disposition.....	63
4. Discussion.....	70
5. Conclusion	78
Bibliography.....	80

ABSTRACT

Lamivudine (3TC) is a negative enantiomer of 2'-deoxy-3'-thiacytidine, which is used in the treatment of hepatitis B virus (HBV) infection. It is desirable to selectively deliver the antiviral drugs used in the treatment of HBV infection to their site of action (liver). In this study, a liver-selective dextran prodrug (3TCSD) of the antiviral drug lamivudine (3TC) was developed and characterized. 3TC was coupled to dextran (~25 kDa) using a succinate linker, and the in vitro and in vivo behavior of the conjugate was studied using newly-developed size-exclusion and reversed-phase analytical methods. Synthesized 3TCSD had a purity of > 99% with a degree of substitution of 6.5 mg 3TC per 100 mg of the conjugate. Furthermore, the developed assays were precise and accurate in the concentration ranges of 0.125-20, 0.36-18, and 1-50 µg/mL for 3TC, 3TC succinate (3TCS), and 3TCSD, respectively. In vitro, the conjugate slowly released 3TC in the presence of rat liver lysosomes, whereas it was stable in the corresponding buffer. In vivo in rats, conjugation of 3TC to dextran resulted in forty- and seven-fold decreases in the clearance and volume of distribution of the drug, respectively. However, the accumulation of the conjugated 3TC in the liver was fifty-fold higher than that of the parent drug. The high accumulation of the conjugate in the liver was associated with a gradual and sustained release of 3TC in the liver. In addition to the liver, kidney was the only other organ where high concentrations of the conjugate were found. In contrast to the liver and kidneys, the concentrations of the conjugate and/or regenerated 3TC were very low or undetectable in the lungs, spleen, and heart after 3TCSD injection. These studies indicate the feasibility of the synthesis of 3TC-succinate-dextran and its potential

use for the selective delivery of 3TC to the liver.

LIST OF TABLES

1	Tissue: plasma AUC ratios of FDs in rats (Mehvar et al., 1994).....	28
2	Relationship between the 3TCSD peak area and the added plasma concentration [Peak area=Intercept + (slope x Conc)] for the SEC method	53
3	Inter-run accuracy and precision for quantitation of 3TCSD using the SEC assay ($n = 5$).....	53
4	Relationship between analyte: internal standard peak area ratio and the added plasma concentration [Peak area=Intercept + (slope x Conc.)] for reversed-phase method.....	56
5	Inter-run accuracy and precision for quantitation of 3TC and 3TCS in plasma using the reversed-phase assay ($n = 5$)	56
6	Plasma Pharmacokinetic Parameters (Mean \pm S.D.) of Unconjugated (3TC) and Dextran-Conjugated (3TCSD) Lamivudine after a Single iv Dose (5 mg/kg, 3TC Equivalent) of 3TC or 3TCSD	64
7	Ratios of the regenerated 3TC AUC after 3TCSD over parent 3TC AUC after 3TC in all the studied tissues after iv administration of single, 5-mg/kg doses (3TC equivalent) of 3TC or 3TCSD to rats.....	69

LIST OF FIGURES

1	Chromatograms of plasma samples taken from a rat before (A) and 180 min after (B) the administration of a single 5-mg/kg dose (3TC equivalent) of 3TCSD, subjected to the size-exclusion chromatographic method. The 180-min sample contained 9.70 $\mu\text{g/mL}$ of 3TCSD.	52
2	Chromatograms of plasma samples taken from a rat before (A) and 15 min after (B) the administration of a single 5-mg/kg dose of 3TC to rats and at 3 h after in vitro incubation of 3TCSD with rat blood (C), subjected to the reversed-phase chromatographic method. Sample B contained 1.84 $\mu\text{g/mL}$ of 3TC and sample C contained 3.97 and 5.12 $\mu\text{g/mL}$ of 3TC and 3TCS, respectively.	55
3	Average concentration-time courses of the intact 3TCSD (top) and released 3TC, 3TCS, and total 3TC (3TC plus 3TCS) (bottom) after incubation of the conjugate at pH 4.4 (37 $^{\circ}\text{C}$). Error bars represent S.D. values ($n = 3$). Error bars for 3TCSD are too small to be observable.	58
4	Average concentration-time courses of the intact 3TCSD (top) and released 3TC, 3TCS, and total 3TC (3TC plus 3TCS) (bottom) after incubation of the conjugate at pH 7.4 (37 $^{\circ}\text{C}$). Error bars represent S.D. values ($n = 3$). In most cases, error bars are too small to be observable.	59
5	Average concentration-time courses of the intact 3TCSD (top) and released 3TC, 3TCS, and total 3TC (3TC plus 3TCS) (bottom) after incubation of the conjugate in rat blood (37 $^{\circ}\text{C}$). Error bars represent S.D. values ($n = 3$). In most cases, error bars are too small to be observable.	61
6	Average concentration-time courses of released 3TC after incubation of the conjugate in rat liver lysosomes or buffer (37 $^{\circ}\text{C}$) at pH 4.0. Error bars represent S.D. values ($n = 3$). In most cases, error bars are too small to be observable.	62
7	Plasma concentration-time courses of the conjugated (3TCSD) and unconjugated (3TC) lamivudine after iv administration of single, 5-mg/kg doses (3TC equivalent) of 3TC or 3TCSD to rats. Standard deviation values are shown as error bars ($n = 3$ rats for each point).	63
8	Liver concentration-time courses (top) and AUC values (bottom) of parent (3TC) and/or conjugated (3TCSD) lamivudine after iv administration of single, 5-mg/kg doses (3TC equivalent) of 3TC or 3TCSD to rats. Standard deviation values are shown as error bars ($n = 3$ rats for each time point). Asterisks indicate significant differences from the other two groups.	67
9.	Kidney concentration-time courses (top) and AUC values (bottom) of parent (3TC) and/or conjugated (3TCSD) lamivudine after iv administration of single, 5-mg/kg doses (3TC equivalent) of 3TC or 3TCSD to rats. Standard deviation values are shown as error bars ($n = 3$ rats for each time point). Asterisks indicate significant differences from the other two groups.	69

CHAPTER I

INTRODUCTION

Hepatitis B is a serious liver disease caused by hepatitis B virus (HBV). The virus can cause lifelong infection, cirrhosis (scarring) of the liver, liver cancer, liver failure, and death. Hepatitis B virus (HBV) infection, with more than 350 million carriers worldwide, remains a difficult public health problem in spite of decades of research into various modes of treatment (Dumas et al., 2007). It is generally believed that HBV in itself is not hepatotoxic; but it is the immune response to the virus that is hepatotoxic. The various stages of acute HBV infection in adults and children older than 6 years can be divided into 3 groups. The first stage, called the replicative stage, is characterized by seropositivity for hepatitis B e antigen (HBeAg), high HBV DNA levels, and high transaminase levels, the rise in transaminase levels reflecting the host immune response to the virus. This is usually followed by loss of HBeAg, development of anti-HBe antibodies, reduction of HBV DNA levels, and normalization of transaminases. The second stage is known as the inactive carrier stage. The third stage, resolution of the infection, is characterized by hepatitis B surface antigen (HBsAg) loss and anti-HBsAg seroconversion (Dumas et al., 2007).

The main clinical result is the development of chronic hepatitis, followed by liver cirrhosis and hepatocellular carcinoma. Long term viral suppression should be the principal goal of antiviral therapy and also to improve the clinical outcome of

the patients (Zoulim, 2006).

The therapeutic end points, one year after anti-viral therapy include the following: (1) Viral suppression reflected by loss of HBeAg with or without seroconversion to anti-HBe and a decrease in HBV DNA. (2) Reduction in liver damage, reflected by the return to normal values of serum aminotransferases (if these are high) and by histological improvement on liver biopsy samples. The ultimate long-term aim in the treatment of patients with chronic hepatitis infection is to prevent or at least to minimize the risk of the development of cirrhosis and hepatocellular carcinoma (Yuen and Lai, 2001).

1.1. Goals of antiviral therapy

The main aim of antiviral therapy is to suppress HBV replication and to induce the remission of liver disease activity. The inhibition of HBV replication reduces the patient's infectivity and subsequently the risk of HBV transmission. In patients with wild type virus infection, the primary goal of antiviral therapy is to achieve seroconversion from HBeAg to the homologous anti-HBe antibody (HBe seroconversion) as this immunologic event is associated with a reduction of the risk of progression of the liver disease (Zoulim, 2006).

The need for treatment of hepatitis B depends on the history of the disease. The progression of the infection to cirrhosis and hepatocellular carcinoma depends on the state of the immune system, the age of the patient, the serologic stage of infection, and other issues like geographic and genetic factors (Lee, 1997). The main objective of antiviral therapy is to control viral replication, to decrease or

prevent ALT flares and/or induce remission of disease. The virological response is manifested if the HBV DNA levels decline below 10^4 or 10^3 copies/mL in blood. The biological response is defined by the normalization of ALT levels, and the histological response is defined by the improvement in the fibrosis indices or inflammatory activity.

1.2. Agents for the treatment of chronic hepatitis B

The agents currently used or which are under investigation for the treatment of chronic hepatitis B can be broadly divided into two main groups, immunomodulators and nucleoside analogues.

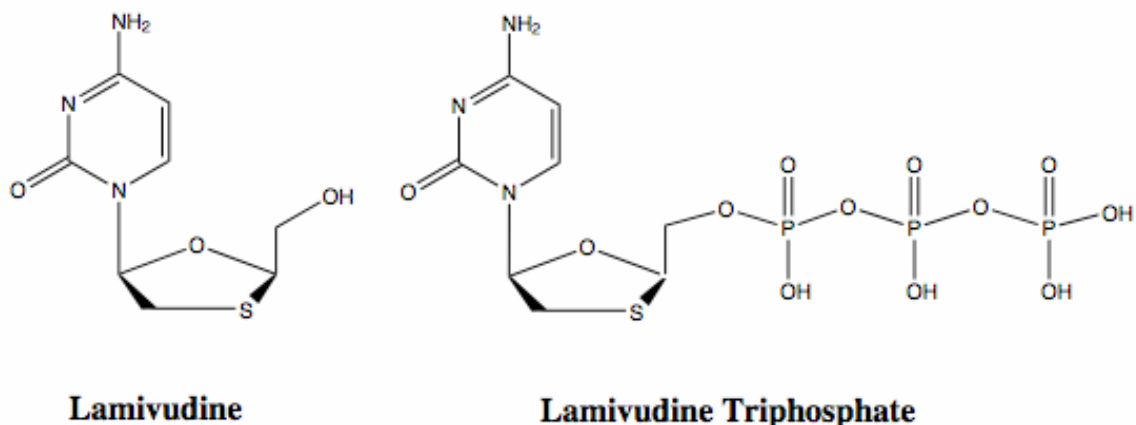
Immunomodulators act on the immune response of the host to HBV antigens expressed on the surface of the infected liver cells, causing or potentiating the lysis of infected hepatocytes. Interferon α is the principal agent among this class of drugs and is the first agent to be approved for use as an anti-hepatitis drug. It is given parenterally (subcutaneously) in a 16-week course of either 5 million units (MU) daily or 10 MU three times per week. Factors associated with poor response to interferon α include male sex, long duration of infection, Asian origin, low alanine aminotransferase concentrations, high HBV DNA concentrations, liver histology showing low to mild activity, and impaired immunity. Additionally, the drug has significant side effects, such as influenza like syndrome, myalgia, bone marrow suppression, alopecia, depression, and induction of autoantibodies. In patients with advanced hepatitis/cirrhosis the drug may cause susceptibility to bacterial infection and worsening of liver functions. These adverse effects can be severe and

debilitating and are generally dependent on the dose. Most of the adverse effects can be decreased by lowering the dose of interferon α , but some of them require premature termination of therapy (Yuen and Lai, 2001). Other novel agents of this class (Immunomodulators) include pegylated interferon, thymosin α , and therapeutic vaccines.

The second group of agents, which are also the preferred drugs for the treatment of chronic hepatitis B, is the nucleoside analogues. These act by inhibiting the replication of the virus and hence prevent reinfection of healthy hepatocytes. It is also believed that, indirectly, they may enhance immune clearance of infected hepatocytes (Yuen and Lai, 2001). The major drugs in this group include lamivudine, adefovir dipivoxil, and entecavir, with lamivudine being the most widely investigated and used for the treatment of HBV infection.

1.3. Lamivudine

Lamivudine (3TC) (Scheme 1) is a novel cytosine nucleoside analogue, reverse transcriptase inhibitor used in the treatment of infections caused by hepatitis B virus (HBV) or human immunodeficiency virus type 1 (HIV-1) (Johnson et al., 1999). It is the negative enantiomer of 2'-deoxy-3'-thiacytidine (Soudeyns et al., 1991). The negative enantiomer of lamivudine is less toxic than its positive enantiomer (Coates et al., 1992b). Lamivudine is converted to its active form in the hepatocytes, where stepwise addition of phosphate groups yields the active 5'-triphosphate form (Scheme 1) (Yuen and Lai, 2001).



Scheme 1: Chemical structures of lamivudine and its active form (lamivudine triphosphate).

Studies in peripheral blood mononucleocytes (PBMCs) have shown that the drug is converted initially to its monophosphate form by deoxycytidine kinase, followed by conversion to its diphosphate form by cytidine monophosphate kinase and deoxycytidine monophosphate kinase and ultimately to its active triphosphate form by pyrimidine nucleoside diphosphate kinase (Cammack et al., 1992). The rate-limiting step in the conversion of lamivudine to its active triphosphate form is the formation of the predominant anabolite lamivudine diphosphate (Moore et al., 1999a).

In *in vitro* tests (Soudeyans et al., 1991; Coates et al., 1992a; Coates et al., 1992b), lamivudine has shown to be active against a wide range of retroviruses. In these tests (Soudeyans et al., 1991; Coates et al., 1992b), the 50% inhibitory concentration (IC₅₀) of lamivudine against HBV (hepatic cell lines) ranged from 4 to 7 µg/L (0.018 to 0.032 µmol/L) (Furman et al., 1992); Chang, 1992 #270]. The main mechanism of action of lamivudine is by suppressing or inhibiting the

replication of HBV. Lamivudine shows two modes of viral suppression. First, the active triphosphate metabolite mimics deoxycytidine triphosphate and is incorporated into newly synthesized viral DNA, causing chain termination. Second, the active triphosphate form competitively inhibits viral DNA-dependent and RNA-dependent DNA polymerase (reverse transcriptase) activity (Yuen and Lai, 2001).

After a year of therapy, lamivudine treatment reduces the viral load by 3-5 \log_{10} copies/mL, compared to baseline values. Lamivudine treatment also reduces the ALT levels significantly and leads to the improvement of the histology activity index. Improvement in liver fibrosis has also been reported with lamivudine therapy (Yuen and Lai, 2001).

The major drawback in the use of lamivudine as a single agent is the emergence of resistance due to the development of mutant strains of HBV (Yuen and Lai, 2001). Spontaneous variability of HBV genome and the slow kinetics of viral clearance are believed to be the biological basis for drug resistant mutants. Moreover, a low (below inhibitory concentrations) drug level at the site of action (hepatocytes) because of once-daily administration has been suggested to cause resistance (Bernasconi, 1998). Phase III clinical trials have shown the incidence of lamivudine resistance to be about 20% per year. *Lai et al.* have shown that lamivudine resistance develops in up to 70% of patients after four years of therapy. Lamivudine resistance causes an increase in viral load (viral breakthrough), which is followed by an increase in the ALT levels (biochemical breakthrough), reduced HBe seroconversion rate, and progression of liver disease (Zoulim, 2006).

Resistance causing mutations to lamivudine are mainly located in the C domain of the reverse transcriptase within the YMDD motif (Zoulim, 2006).

1.3.1. Pharmacokinetics

After both oral and intravenous administration, lamivudine shows a linear, dose-independent pharmacokinetic profile, with C_{max} and AUC values reflecting the magnitude of the dose. In a study (Moore et al., 1999b), it was demonstrated that single dose, multiple dose, and population pharmacokinetic studies are not significantly dependent on either race or gender. The absolute bioavailability of lamivudine is lower and systemic clearance is greater in children with HIV-1 infection who are younger than 12 years when compared to older children and adults (Lewis et al., 1996). The pharmacokinetic profile in women with HIV-1 during late pregnancy or labor was not significantly altered when compared to the profile in non-pregnant women (Johnson et al., 1999).

1.3.1.1. Absorption

Lamivudine shows high water solubility and is a highly permeable drug showing rapid dissolution rates. As a result, oral doses are rapidly absorbed through passive diffusion across the intestinal wall. The average time to reach C_{max} ranges from 0.5 to 1.5 hours following oral doses. Additionally, the absolute bioavailability of lamivudine, which is not affected by dose, is approximately 82% (van Leeuwen et al., 1992). The geometric least square (GLS) mean C_{max} and AUC values of lamivudine after a 100 mg oral dose (recommended for patients with HBV

infection) were 1002 $\mu\text{g/L}$ (95% CI, 860 to 1167 $\mu\text{g/L}$) and 3781 $\mu\text{g/L}\cdot\text{h}$ (95% CI, 3505 to 4079 $\mu\text{g/L}\cdot\text{h}$), respectively (Yuen et al., 1995).

1.3.1.2. Effect of food on absorption

The effect of food on the pharmacokinetics of lamivudine has been evaluated in two different clinical trials (Moore et al., 1999b). In the first study, *Angel et al.* (Angel, 1993) administered a small, 50 mg single oral dose to 12 men with HIV-1 infection after an overnight fast or immediately after a standard fat meal. The meal did not significantly alter the total amount of drug absorbed into the systemic circulation, as judged by comparable values of 24-hour AUCs (1548 \pm 247 and 1677 \pm 424 $\mu\text{g/L}\cdot\text{h}$) and fraction of lamivudine excreted in the urine over 24 hours (68.6 \pm 11 and 69.7 \pm 10%) in the fed and fasting states, respectively. However, intake of food had a significant impact on the mean C_{max} by reducing it by 47% [273 \pm 56 $\mu\text{g/L}$ (fed) vs. 513 \pm 215 $\mu\text{g/L}$ (fasting)] and also delayed the mean time to reach C_{max} (t_{max}) by 2.25 hours [3.2 hours (fed) vs. 0.9 hours (fasting)].

1.3.1.3. Distribution

Lamivudine shows wide distribution to various tissues beyond the systemic circulation [Johnson, 1999 #73]. Over the intravenous dosing range of 0.25 to 8 mg/kg, the mean apparent volume of distribution (V_d) of lamivudine is approximately 1.3 L/kg (van Leeuwen et al., 1992), indicating that the drug is being distributed into the total body fluid. The oral apparent volume of distribution (V_d/F) of lamivudine is dose-dependent and does not show any relationship with the

bodyweight. The wide volume of distribution of lamivudine may be partly due to its relatively low molecular weight (229 Da) and low plasma protein binding (<36%). *In vitro* studies have shown that the plasma protein binding of lamivudine is dependent on the concentration, with approximately 35 to 50% at plasma concentrations around 100 µg/L and <10% at concentrations of ≥ 1000 µg/L. Over the concentration range of 0.1 to 100 mg/L, lamivudine distribution into erythrocytes ranges from 53 to 57%, which is concentration-independent (Johnson et al., 1999).

1.3.1.4. Metabolism and elimination

Metabolism of lamivudine is a minor route of elimination. Approximately 5 to 10% of the parent compound undergoes metabolism to its pharmacologically inactive trans-sulphoxide metabolite, a major portion of it is excreted into the urine within 12 hours after a single oral dose. Serum concentrations of this metabolite have not yet been determined. Lamivudine does not undergo any phase-II metabolism like glucuronide conjugation. Around 70% of the drug is eliminated unchanged in the urine over 24 hours (Heald et al., 1996). It was observed that renal clearance (CL_R) of lamivudine is greater than its glomerular filtration, indicating that lamivudine is eliminated by filtration and active renal tubular secretion (Johnson et al., 1999).

1.3.1.5. Effect of hepatic dysfunction

The pharmacokinetic profile of lamivudine in patients with moderate to severe hepatic impairment is not much different when compared to patients with normal hepatic function (Johnson et al., 1998). Thus, the stage of hepatic damage and fibrosis, whether induced by HBV or alcohol-induced cirrhosis, is not likely to have a significant impact on lamivudine exposure or efficacy. *Johnson et al.* investigated the pharmacokinetics of lamivudine in patients with end-stage chronic HBV infection who were undergoing liver transplantation and maintained on lamivudine for up to 3 months after the transplant. Lamivudine 100 mg once daily was given before and after transplant and 3 times daily at the time of transplant, with day 1, day 14, and 3 month pharmacokinetic assessment being performed in 22, 17, and 11 patients, respectively. Median values for lamivudine CL/F (17.6, 17.2, and 13.9 L/h at day 1, day 14, and month 3 evaluations, respectively) and pre- and post-transplant t_{max} , C_{max} , and $t_{1/2\beta}$ estimates were consistent with values reported in patients with normal hepatic function. Lamivudine AUC values (5690, 5826, and 7220 $\mu\text{g/L}\cdot\text{h}$ at day 1, day 14, and month 3 evaluations, respectively) were approximately 50% higher than values reported in non-hepatically impaired patients. This increase in AUC may be due to the decrease in the CL_R in patients after liver transplant (Johnson et al., 1999).

Hepatic impairment has an effect in the production of the pharmacologically inactive trans-sulphoxide metabolite of lamivudine. Since metabolism accounts for a minor role in the elimination pathway of lamivudine, the pharmacokinetics of

lamivudine is unlikely to be altered and is unlikely to have any meaningful clinical effect (Johnson et al., 1999).

1.3.1.6. Effects of renal dysfunction

The pharmacokinetics of lamivudine is significantly affected in patients with renal insufficiency. In a study (Heald et al., 1996), the pharmacokinetics of lamivudine in patients with normal, moderate, and severe renal impairment were compared after a single 300 mg oral dose. The results showed that compared with normal renal function, patients with moderate and severe renal impairment had, respectively, 4- and 13-fold higher mean lamivudine AUC values, 1.2- and 1.8-fold longer $t_{1/2\beta}$ values and one-eighth and one-hundredth of renal clearance values. Because of this drastic change in the pharmacokinetic parameters, the dosage should be lowered in these patients, in order to achieve drug levels similar to patients having normal renal function.

1.3.1.7. Multiple dose pharmacokinetics

Multiple dose studies were conducted in HBV infected patients, aged 16-65 years. These patients randomly received 5, 20, 100, 300, or 600 mg once daily dose of lamivudine or as twice daily (n=12) regimens for 15 days. Blood samples were collected up to 12 and 24 hours, post dosing. In both studies, day 1 and 15 values for C_{\max} and t_{\max} were identical. Day 15 values for AUC were significantly larger than AUC values for day 1, after twice daily administration, perhaps due to accumulation of the drug over 15 days. Dose proportionality was observed in the

pharmacokinetics of lamivudine, reflected by a corresponding increase in the AUC and C_{\max} of lamivudine, as the dose was increased from 5 mg/day to 600 mg/day on days 1 and 15.

1.3.1.8. Drug interactions

Isolated perfused rat kidney experiments were performed (Sweeney et al., 1995) to investigate potential drug interactions between lamivudine and 8 other drugs. Lamivudine was maintained at a concentration of 500 $\mu\text{g/L}$ in the perfusate, in the presence of zidovudine 1 mg/L, zalcitabine 2 mg/L, didanosine 1 mg/L, probenecid 50 mg/L, sulphamethoxazole 80 mg/L, trimethoprim 4 mg/L, or cimetidine 2 mg/L. CL_R and extraction ratio of lamivudine were significantly reduced by trimethoprim, while zalcitabine significantly reduced the extraction ratio. The other 6 drugs did not show any interactions with lamivudine.

Lamivudine shows low metabolic clearance and low plasma protein binding. These properties suggest that there is little potential for drug-drug interactions with drugs which show high plasma protein binding and/or drugs which are metabolized. Drugs whose main elimination pathway is through kidneys and are actively secreted (primarily by the organic cationic transporter system) may have the potential to cause interactions with lamivudine (Johnson et al., 1999).

1.3.2. Adverse effects

Common adverse effects like diarrhea, dizziness, occurred in less than 17% of the patients (Jarvis and Faulds, 1999). A recent study was performed in 358

patients infected with chronic HBV infection, receiving lamivudine 25 mg (n=142), 100 mg (n=143), or placebo (n=73) for 1 year. It was found that the incidence of adverse effects and overall tolerability were not much different between these two groups (Lai et al., 1998). There was no relation between lamivudine treatment and significant elevations in serum alanine, aspartate aminotransferase, creatinine kinase, amylase or other hematological or biochemical variables (Johnson et al., 1999).

Lamivudine exhibits little cytotoxic effects towards human cell lines and does not interfere with the synthesis of human DNA (Gray et al., 1995). Lamivudine does not cause inhibition of mitochondrial DNA even at therapeutic concentrations of 0.01 to 0.03 $\mu\text{mol/L}$ (Chang et al., 1992).

It is generally believed that delayed mitochondrial toxicity is the mechanism which causes adverse effects associated with nucleoside analogues (Cui et al., 1995; McKenzie et al., 1995; Schalm et al., 1995; Swartz, 1995). To test whether lamivudine causes any delayed mitochondrial toxicity, the structure and function of hepatocellular mitochondria was investigated in 15 patients receiving 25 to 300 mg per day for the treatment of chronic hepatitis B. It was concluded (Honkoop et al., 1997) that no evidence of mitochondrial toxicity was found during the study period of 24-weeks.

Lamivudine is better tolerated than interferon- α (alone or in combination with lamivudine). In various comparative tests, the frequency of common adverse effects like hair loss, malaise, and fever was 2 to 8 times more likely to occur in

patients treated with interferon- α (alone or in combination with lamivudine) than lamivudine. Also, abnormal liver functions occurred in 10% of patients treated with lamivudine alone, in 14% of patients receiving interferon- α , and in 9% of patients treated with a combination of lamivudine and interferon- α (Jarvis and Faulds, 1999).

1.3.3. Dosage and administration

For patients with chronic hepatitis B with active HBV replication and liver inflammation, the recommended daily dose of lamivudine is 100 mg. For patients co-infected with HIV, a higher dose of 150 mg twice daily is recommended, in combination with other anti-retrovirals (Jarvis and Faulds, 1999).

It is of importance that treatment of lamivudine in patients with unrecognized or untreated HIV infection will lead to the emergence of lamivudine-resistant HIV and limit treatment options for HIV. Therefore, it is recommended that proper testing be offered to patients before and during the course of treatment. An important advantage of lamivudine is that it can be administered with or without food, which facilitates changes in the drug administration schedule in the patient (Jarvis and Faulds, 1999).

1.3.4. Place of lamivudine in the management of chronic hepatitis

B

The mechanism of action of lamivudine involves the inhibition of replication of HBV by interfering with viral DNA polymerase.. There are profound

reductions in the HBV DNA levels in a patient when treated with lamivudine. Significant improvements in liver histology and normalization of ALT levels were more common in lamivudine than the placebo group in several clinical trials in patients with ongoing viral replication, including HBeAg-negative patients- a group that generally does not respond to interferon- α (Lai et al., 1998; Tassopoulos et al., 1999).

It was observed that within 1 year of lamivudine treatment, significant improvements in liver histology were observed in a large patient population (Lai et al., 1998; Tassopoulos et al., 1999). Hepatic necroinflammatory activity was reduced and the progression to hepatic fibrosis was halted or reversed in patients under lamivudine treatment. An important clinical feature of lamivudine is that lamivudine arrests the progression of hepatic fibrosis to cirrhosis (Jarvis and Faulds, 1999).

In conclusion, lamivudine inhibits HBV replication in patients with chronic hepatitis B infection, irrespective of ethnicity, mode of acquisition of the virus, or the presence of wild type or mutant HBV. The drug attenuates hepatic necroinflammatory activity and the progression of fibrosis in patients with chronic hepatitis B, active viral replication and severe liver disease. The drug shows good tolerability in patients and does not cause any serious drug-drug interactions. Overall, lamivudine is a very useful drug in a wide spectrum of patients having chronic hepatitis B (Jarvis and Faulds, 1999).

1.4. Drug delivery approaches in Hepatitis B treatment

Because of the localization and replication of HBV mainly occurs in the liver, there have been numerous efforts by various scientists to target anti-viral agents selectively to the liver using different approaches. The following section will give a brief overview of the various ways in which different anti-viral agents have been conjugated to different substances to selectively target them to the liver.

1.4.1. Macromolecular prodrug approaches

These approaches rely on targeting of the antiviral drugs to the liver by conjugating the drug with a macromolecule that actively or passively accumulates in the liver. Once in the liver, the prodrug is expected to release the drug slowly, resulting in selective accumulation and prolonged release of the drug in the liver.

1.4.1.1. Protein and glycoprotein carriers

Rabbit serum albumin (RSA) was used as a macromolecule via a carbodiimide bond to conjugate two inhibitors of DNA synthesis, 5-Fuoro-deoxyuridine (FUDR) and cytosine arabinoside (ara-C). Phosphorylation of the primary hydroxyl groups releases the free drug from the conjugate, which in turn inhibits DNA synthesis. *In vitro* experiments were performed (Barbanti-Brodano and Fiume, 1974; Balboni et al., 1976) to test the potential of FUDR-RSA and ara-C-RSA in killing (pinocytosing) and proliferating cells. Mice infected with *Ectromelia* virus, the agent causing mouse pox, were chosen to test the anti-viral activity of these macromolecules. The anti-viral activity of FUDR-RSA and ara-C-

RSA was evaluated based on the inhibition of virus production in the liver and the survival time and number of survivors. The conjugates, injected into mice at the same time as that of virus, reduced the virus yield in liver by 1-2 logs 48 h after injection. On the other hand, free FUDR and ara-C after injection into infected mice were completely ineffective in decreasing the virus yield in the liver. Also, ara-C-RSA significantly increased the mean survival time of infected mice and also increased the number of survivors. The conjugates were active only when administered 12 to 24 h after infection. These results conclude that conjugation of anti-viral agents with macromolecules like rabbit serum albumin can be used to selectively target drugs and enhance the anti-viral activity when compared with the free parent drug.

In another approach (Fiume et al., 1979), Trifluorothymidine (F_3T), an inhibitor of DNA synthesis, was coupled to glycoproteins for active targeting to the liver cells via asialoglycoprotein receptors. Coupling of the drug was achieved by treating glycoproteins to remove sialic acid and to expose the galactosyl residues. F_3T was converted to glutarate and was subsequently coupled to the $-NH_2$ group of asialofectin (AF, a glycoprotein) via a hydroxysuccinimide ester. The coupling of F_3T did not change any properties of AF, like its ability to interact with specific receptors on hepatocytes. To test the anti-viral activity of F_3T and F_3T -AF *in-vivo*, they were administered into mice, 44 h after *Ectromelia* infection. The anti-viral activity was evaluated based on deoxycytidine incorporation into DNA, and was determined in liver and in bone-marrow. F_3T -AF was 3 times more effective in

inhibiting deoxycytidine incorporation into DNA than compared with equal doses of free F₃T. On the other hand inhibition of deoxycytidine incorporation in the bone marrow was to the same extent for the free drug and conjugated F₃T.

In a similar approach (Fiume et al., 1980), a different anti-viral agent, adenine-9-β-D-arabinofuranoside (ara-A), which is less toxic than F₃T, was coupled to AF. Two different approaches were used to conjugate Ara-A with AF. In the first approach, glutarate of ara-A was coupled to –NH₂ group of AF via hydroxysuccinimide ester. In the second approach, ara-A was phosphorylated to its mono-phosphate (ara-AMP), and was coupled to AF via a water soluble carbodiimide. The anti-viral activity of the drug was evaluated based on its ability to inhibit thymidine incorporation into DNA in liver and intestines. To test the efficacy *in-vivo*, free ara-A, free ara-AMP and ara-A conjugate were administered 44 h after *Ectromelia* virus infection in mice. Free ara-A and free ara-AMP produced greater inhibition of DNA synthesis in the intestines, compared with that in the liver. On the other-hand, AF-ara-A conjugates produced substantial inhibition of DNA synthesis only in the liver.

The major drawback in the use of AF conjugates is their immunogenicity (Fiume et al., 1982a). Immunogenicity causes induction of antibodies which produces allergic reactions in the body. This problem can be overcome by the use of lactosaminated homologous (from same species) albumin as a hepatotropic carrier of drugs (Fiume et al., 1988). Lactosaminated serum albumin (L-SA) enters specifically into hepatocytes by binding to the galactosyl-terminating glycoprotein

receptors (Fiume et al., 1988). L-SA-ara-A conjugates were synthesized (Fiume et al., 1981; Fiume et al., 1982b) using rabbit and human L-SA and the coupling of ara-A was via a carbodiimide bond. Anti-viral activity of conjugated Ara-A and free ara-A was tested in *Ectromelia* infected mice. In mice administered with free ara-A, inhibitions of DNA ranged from 25-50% in the liver, 31-62% in intestines, and 0-43% in the bone marrow. In animals injected with L-SA-ara-A conjugate, DNA synthesis inhibition ranged from 21-58%, 0-23%, and 0-2% in the same organs, respectively. The amounts of drug required to inhibit DNA synthesis in the liver was about 10 fold lower when ara-A was administered as a conjugate when compared to free ara-A administration. In subsequent tissue distribution studies, it was found that L-SA-ara-A conjugates exclusively accumulated in the liver. Very small quantities of the conjugate were found in intestines, spleen and kidneys. These results conclude beyond doubt that anti-viral agents can be selectively delivered to organs by conjugation with protein carriers.

1.4.1.2. Poly L-lysine carriers

A conjugate of antiviral drug, adenine arabinoside monophosphate (ara-AMP) was synthesized with a lactosaminated poly-L-lysine (Fiume et al., 1994; Fiume et al., 1995). The first step in the synthesis of the conjugate involved the lactosamination of poly-L-lysine. Lactosamination was followed by the conjugation of the polymer with the antiviral agent ara-AMP via a carbodiimide ester. To test the antiviral activity of the conjugate *in vivo*; (Fiume et al., 1995; Fiume et al., 1997a), 5.8 mg/kg (2.5 mg/kg, ara-AMP equivalent) was injected IM in three

woodchucks, one daily for 37 days. It was observed that, during treatment, woodchuck hepatitis viral DNA (WHV DNA) fell to undetectable levels by the dot-blot hybridization technique. However, low levels of WHV DNA were detected in the last days of treatment with the conjugate, and viraemia levels rose when treatment was stopped.

To test whether the carrier had any toxic effects at high concentrations when administered *in vivo*, a single injection of 375 mg/kg of L-Poly (Lys)-ara-AMP was administered i.v. to rats (Fiume et al., 1997a). The body weight gains were measured at 3, 8, and 14 days after drug administration. It was observed that the gain in the body weight was similar in the treatment and the control groups. Therefore, it can be concluded that administration of high doses of the conjugate did not produce any toxicity in rats.

In another study (Di Stefano et al., 1997a), ribavirin (RBV), which is a broad spectrum anti-viral agent, was conjugated with lactosaminated poly-L-lysine. The main drawback of ribavirin is the accumulation in erythrocytes causing haemolysis (Catlin DH, 1980; Laskin et al., 1987; Brillanti et al., 1994; Chemello et al., 1995; Main, 1995; Lai et al., 1996; Schalm et al., 1997). Conjugation is thought to reduce the accumulation significantly in erythrocytes and also help in the targeted delivery of the drug to the liver.

Conjugation of ribavirin (Di Stefano et al., 1997b) was achieved by coupling ribavirin monophosphate (RBVMP) to L-poly (LYS) preparation in which amino groups have been substituted with lactose residues. To test the liver targeting

potential and anti-viral efficacy of the conjugate, *in vivo* studies were performed in mice. Administration of the conjugate lead to a 2.2 or 4.7 fold higher levels of the drug in the liver when compared to the administration of free RBV, administered intramuscularly or orally, respectively. 2-fold higher concentration of RBV-triphosphate was found in mice administered with the conjugated drug than in animals orally treated with free RBV. Also, conjugation of RBV decreased the ED₅₀ of RBV from 47.2 µg/g to 27.4 µg/g. These results (Di Stefano et al., 1997b) show that conjugation of RBV decreases the haemolysis caused by free RBV without compromising on the pharmacological properties of the drug.

1.4.1.3. Polysaccharide carriers

1.4.1.3.1. Arabinogalactan

Arabinogalactan is a polysaccharide of arabinose and galactose and has a high affinity for the asialoglycoprotein receptor (Groman et al., 1994). A conjugate of ara-AMP was synthesized and administered *i.v.* into WHV-infected woodchucks at a daily dose of 50 mg/kg (3 mg/kg of ara-AMP equivalent) (Enriquez et al., 1995). The conjugate produced significant decrease in the viraemia levels when compared to the free drug, administered at a dose of 15 mg/kg/day. Toxicity studies performed in rats and mice after administration of high doses, which were several times higher than effective doses, did not produce any toxic effects or modifications in woodchucks.

The advantage that arabinogalactan has over other hepatotropic carriers is that it does not require any chemical changes in order to bind to the

asialoglycoprotein receptor (Fiume and Verme, 1997).

1.4.1.3.2. Dextrans

Recently, a dextran-acyclovir conjugate was synthesized (Tu et al., 2004) to specifically target acyclovir to the liver and increase the liver distribution of acyclovir through dextran conjugation. The conjugation of acyclovir with dextran (40 kDa) was achieved via an imine bond. Liver targeting potential of dextran-acyclovir or acyclovir alone was tested by administering 65 mg/kg of acyclovir or dextran-acyclovir (acyclovir equivalent) into mice via the tail vein. The results showed that the conjugate accumulation in the liver (AUC of 5494 $\mu\text{g}\cdot\text{h}/\text{g}$) was much higher than the parent drug (AUC of 1397 $\mu\text{g}\cdot\text{h}/\text{g}$). The conjugate also showed appreciable stability in plasma when compared with acyclovir alone. These results proved that dextran conjugation altered the disposition profile of the acyclovir, leading to increased accumulation in the liver and showing appreciable stability in plasma.

1.4.2. Other approaches

In a recent study, a new class of phosphate and phosphonate prodrugs termed *HepDirect prodrugs* (Reddy et al., 2005) were developed. These prodrugs of antiviral drugs require cytochrome P450 for their conversion to the monophosphate form of the drug. Therefore, although their delivery is not selective to any organ, their activation is expected to occur in cytochrome P450 rich organs, such as the liver. Moreover, because of the cytochrome P450-mediated direct conversion of the

prodrug to the monophosphate form of the drug, it by passes the first step in the activation of the drug, which requires deoxycytidine kinase.

A *HepDirect prodrug* of lamivudine monophosphate was synthesized and tested in rats (Reddy et al., 2005). Animals were administered an IV bolus dose of either 230 mg/kg of lamivudine or 30 mg/kg (lamivudine equivalent) *HepDirect prodrug*. Although high levels of lamivudine were observed in the plasma following administration of lamivudine (230 mg/kg), the liver concentrations of lamivudine triphosphate were detectable only at 20 min following drug administration. Rats administered with *HepDirect prodrug* (30 mg/kg, lamivudine equivalent) showed no detectable levels of lamivudine in plasma at all time points examined. However, relatively high levels of lamivudine triphosphate were found in the liver following the prodrug administration. The liver-targeting indices based on lamivudine triphosphate liver: plasma AUC ratios were >2.3 and 0.007 following the administration of *HepDirect prodrug* and lamivudine (, respectively). This shows a >320 -fold increase in the liver targeting of *HepDirect prodrug* relative to lamivudine using this approach.

1.5. Dextran as macromolecular carriers

Dextran are glucose polymers which have been used as plasma expanders for many years (Thoren, 1980). Numerous scientists have investigated dextran as potential macromolecular carriers for delivery of various drugs and proteins, with an aim of increasing the longevity of therapeutic agents in systemic circulation. The increase in longevity of drugs is obtained by longer blood half-lives of high M_w

dextran conjugates of therapeutic agents, compared with the intact drug. The major importance of dextrans as drug carriers has been for targeting drugs to specific sites of action, through passive or active targeting.

The important usage of dextrans has been its ability to increase the *in vitro* stability and decrease the *in vivo* immunogenicity of proteins or enzymes. Dextran conjugates of various drugs act as prodrugs, releasing the active drug *in vivo* (Mehvar, 2000).

It is generally believed that the kinetics of drugs attached to polymers is dictated by the kinetics of the polymer. Therefore, it is prudent to analyze the pharmacokinetics of dextrans as macromolecules.

1.5.1. Physicochemical properties

Dextrans are produced from sucrose by the action of bacteria or from chemical synthesis. The structure of a dextran molecule consists predominantly of linear α -1,6-glucosidic linkage with some degree of branching via 1, 3-linkage (Larsen, 1989). The physicochemical properties of dextrans are dependent on both the degree of branching and M_w distribution of the polymer (Walker, 1978). To illustrate this point, it has been reported (Walker, 1978) that the degree of water solubility of dextrans decrease by an increase in the degree of branching of the macromolecules.

1.5.2. Lack of oral availability of dextrans

Dextrans show negligible oral availability after extravascular administration. The oral bioavailability of fluorescein-labeled dextrans (FDs) with average M_w of 4 kDa (FD-4), 20 kDa (FD-20) and 40 kDa (FD-40) in rats was reported to be <0.004 (Mehvar and Shepard, 1992). The reason for the low bioavailability of dextrans is because the size of the dextran macromolecule blocks their passage through the epithelial junctions or aqueous pores of the gastrointestinal (GI) tract; the radius of the smallest dextran (FD-4) is ~ 1.5 nm (Arturson et al., 1971) which is larger than the aqueous pore sizes of the GI tract (0.35-0.75 nm). It has been reported (Koyama et al., 1996) that after receptor-mediated absorption, dextrans undergo degradation into lower M_w fractions during their passage across the epithelial cells of GI tract. For this reason, dextrans are unsuitable candidates to be used for systemic delivery of polymer-drug conjugates after oral administration.

1.5.3. Plasma kinetics

Molecular weight dependency of the pharmacokinetics of dextrans with average M_w of 4 kDa (FD-4), 20 kDa (FD-20), 40 kDa (FD-40), 70 kDa (FD-70), and 150 kDa (FD-150) using serum and urine samples was determined after administration of a single i.v. dose of 5 mg/kg of the polymer to rats (Mehvar and Shepard, 1992). The concentrations of FD-150, FD-70, and FD-40 were above the limit of quantitation up to 12 h after the dosing. Because of a rapid elimination, concentrations of FD-20 and FD-4 were beyond detection in samples after 3 and 1.5 h, respectively, post dosing. All the kinetic parameters exhibited M_w dependency,

the degree of M_w -dependency varied for different parameters. Renal clearance (CL_R) and volume of distribution (V_{ss}) were affected the most and the least, respectively, by the differences in M_w values.

1.5.4. Renal clearance

The main pathways for renal elimination of dextrans in rats are reported (Chang et al., 1976) to occur mainly through glomerular filtration without any considerable tubular secretion or reabsorption. It was shown (Mehvar and Shepard, 1992) that a sigmoidal relationship exists between the fractional renal clearance values and the logarithm of M_w of FDs, with renal clearance approaching zero for FDs with M_w values of ≥ 40 kDa. On the other hand, FD with the lowest M_w (FD-4) had renal clearance which was similar to creatinine clearance. The sigmoidal relationship observed is in agreement with the theoretical models (Arturson et al., 1971; Chang et al., 1976) of renal excretion of macromolecules based on the pore sizes of the glomerular capillary wall. A similar study reported (Chang et al., 1976) that the differences between the kinetic parameters of dextrans with M_w values of ≤ 20 kDa and those with M_w values of ≥ 40 kDa lies in the size of these macromolecules in relation to the pore sizes of the vascular beds in kidneys. It was reported (Chang et al., 1976) that, in rats, renal clearance of neutral dextrans with a radius of ≤ 2.0 nm ($M_w \sim 10$ kDa) occurred without any dependence on the molecular size. However, the renal clearance of dextrans of larger radii progressively decreased and approached zero at a radius of ≥ 4.4 nm ($M_w \sim 40$ kDa).

1.5.5. Metabolism

Depolymerization of dextrans occurs by the different α -1-glucosidases (dextranases) present in various organs in the body, including liver, spleen, kidney, and the lower part of the GI tract (Rosenfeld and Lukomskaya, 1957; Larsen, 1989). In the human body, the liver and spleen have higher concentrations of dextranases (Larsen, 1989). Various *in vitro* studies (Schacht et al., 1988; Vercauteren et al., 1990) using dextranases have shown that the rate of depolymerization is reduced when dextrans undergo slight chemical modification. Therefore, the *in vivo* degradability of the dextran conjugates with drugs or proteins is completely different from the parent polymer. In the liver, dextrans are eliminated through the bile (Lake et al., 1985), apart from metabolism (depolymerization) by the dextranase enzymes (Schacht et al., 1988; Larsen, 1989). It is shown that both of these elimination pathways appear to be slow. A study (Lake et al., 1985) using isolated perfused rat livers indicated that the bile: perfusate ratio of 70-kDa dextran at steady state was 0.09, showing that elimination through bile is slow (Larsen, 1989). Also, the process of depolymerization appears to be slow in the liver (Schacht et al., 1988; Mehvar, 1997), in spite of the liver having high dextranase activity (Larsen, 1989). Another important characteristic of dextran metabolism in the liver is its dependency on the molecular weight of the polymer dextran. In an *in vitro* study (Mehvar, 1997) using liver homogenates containing enzymes (e.g. dextranases, esterases), it was shown that as the M_w increases, the rate constants for metabolism would also increase; *in vitro* first order rate constants of metabolism for

FD-4, FD-70, and FD-150 were 0.00955, 0.0646, and 0.0715 day⁻¹, respectively.

These results are in conformity with an earlier study (Basedow, 1980) indicating that the decrease in the M_w of a dextran with a M_w of ~90 kDa was faster than that for a M_w of ~9 kDa.

1.5.6. Molecular-weight-and dose-dependent tissue distribution and accumulation

The concentrations of FD-4, FD-20, FD-70, and FD-150 in serum and tissues of rats after single 5 mg/kg doses of each FD were measured (Mehvar et al., 1994). The plasma and renal clearance data and the tissue concentration-time profiles of FDs suggested a significant degree of M_w dependence. The tissue: plasma AUC ratios of dextrans, showed significant MW dependency for all the tissues in which dextrans accumulated (Table 1).

Table 1 : Tissue: plasma AUC ratios of FDs in rats (Mehvar et al., 1994).

Tissues	FD-4	FD-20	FD-70	FD-150
Liver	0.346	15.2	28.8	8.59
Spleen	0.095	1.09	7.95	9.56
Kidney	3.49	1.39	0.230	0.003

For the liver, the ratio increased as the M_w increased from 4 to 70 kDa (Table 1). However, an increase in the M_w from 70 kDa to 150 kDa reduced the liver: plasma ratio considerably. On the contrary, for the spleen, as the M_w increased from 4 to 150 kDa there was a progressive increase in the tissue: plasma ratio. For the kidneys, an increase in the M_w resulted in a consistent decline in the accumulation. The ratios for heart and lung were low at all studied M_w values, while

for the brain, there was no detectable accumulation.

All these studies indicate that the tissue disposition of dextrans is dependent on molecular weight. The majority of the administered doses of lower M_w dextrans are renally excreted while the higher M_w dextrans show substantial accumulation in the liver and spleen. The distribution of dextrans to other tissues like brain, lung, and heart appears to be negligible for all the studied M_w values. This data on the M_w dependency of dextrans could be used for the selection of a particular M_w of dextran in design of dextran-drug conjugates for targeted delivery to specific organs.

1.5.7. Effect of electrical charge on the kinetics of dextrans

Various studies (Nishida et al., 1990; Takakura et al., 1990; Nishida et al., 1991; Yamaoka et al., 1995) have shown that electric charge has a significant impact on the disposition of dextrans. It was demonstrated (Takakura et al., 1990) that positively charged radiolabelled dextrans are rapidly eliminated from the plasma of tumor-bearing mice and accumulate in tissues like the liver. However, on the other hand, negatively charged dextrans persist for a long time in the systemic circulation and have negligible tissue accumulation. The slower elimination of negatively charged dextrans is due to the negative charges on most biological membranes, which block the passage of similarly charged molecules (Nishida et al., 1990; Takakura et al., 1990; Nishida et al., 1991).

1.5.8. Kinetics of dextrans modified for receptor-mediated targeting

It is proposed that dextrans enter cells through fluid-phase endocytosis (Lake et al., 1985) which is a passive phenomenon. However, efforts have been made to chemically modify dextrans for active targeting to specific cells in the liver. *Vansteenkiste et al* (Vansteenkiste et al., 1991) prepared dextrans glycosylated with mono- or tri-D-galactose for receptor-mediated delivery to the liver. After administration to rats, it was observed that the plasma clearance and the liver uptake of the galactosylated dextrans were higher when compared with the native dextrans (Vansteenkiste et al., 1991). The mono-D-galactose substituted dextran 6 kDa accumulated in the hepatocytes of the liver, whereas non-galactosylated dextrans mostly accumulated in Kupffer cells. The mechanism behind the liver uptake may be due to the interaction between the galactose terminal on the glycosylated dextran and the hepatic asialoglycoprotein receptor on the hepatocytes membranes, resulting in the uptake of the mono-D-galactosylated dextran into the liver cells. On the contrary, tri-D-galactosylated dextran may not interact with the receptor because of steric differences. In another study (Nishikawa et al., 1993), it was reported that carboxy-methyl dextran (CMD) modified with galactose and mannose residues accumulated mostly in the parenchymal and non-parenchymal cells of the mouse liver, respectively. However, non-modified CMD did not accumulate in either type of cells. This cell-selective accumulation is credited to the galactose and mannose receptors on the parenchymal and non-

parenchymal cells, respectively.

1.6. Hypothesis and specific Aims

In addition to the efficacy of antiviral drugs against HBV, treatment of HBV infection is significantly dependent on the pharmacokinetics of these drugs, in particular their distribution and accumulation in the liver. Based on the above discussion, we hypothesized that a dextran conjugate of lamivudine substantially accumulates in the liver, where it gradually releases the active drug. Such a selective and sustained delivery may necessitate administration of smaller doses of the antiviral drugs, which may be effective for longer periods of time. Additionally, a sustained delivery of lamivudine at the site of action may reduce the incidence of resistance to the drug by maintaining the concentrations of the drug at above inhibitory levels for prolonged periods. Although adverse effects of lamivudine are generally mild, such a delivery approach also has the potential to reduce side effects of other more toxic antiviral drugs in non-target tissues.

Specifically, the aims of the current thesis were:

- To synthesize and characterize a conjugate of lamivudine with dextran 25 kDa using a succinate linker between the drug and the carrier.
- To develop analytical methods for quantitation of the intact prodrug and simultaneous quantitation of its potential release products (lamivudine and lamivudine succinate) in aqueous and biological samples.
- To characterize the in vitro release of the drug in buffers, rat liver lysosomes, and rat blood.
- To determine the plasma pharmacokinetics and tissue disposition of the

conjugate in rats.

CHAPTER II

MATERIALS AND METHODS

2.1. Chemicals

Dextran with an average Mw of 23,500 Dalton was purchased from Dextran Products (Scarborough, Ontario, Canada). Lamivudine (3TC) was purchased from Kemprotec (Middlesbrough, U.K.). Stavudine was purchased from Sigma Chemical (St. Louis, MO). For Chromatography, HPLC grade acetonitrile (Mallinckrodt Chromar HPLC) was obtained from VWR Scientific (Minneapolis, MN). All other reagents were analytical grade and obtained through commercial sources.

2.2. Animals

Adult, male Sprague-Dawley rats were used in this study for in vitro blood and liver lysosomes and in vivo disposition studies as outlined in the subsequent sections. All the procedures involving animals in this study were consistent with the “Principles of Laboratory Animal Care” (NIH publication Vol. 25, No. 28, revised 1996) and approved by the Texas Tech University Health Sciences Center Institutional Animal Care and Use Committee.

2.3. Synthesis of 3TC-succinate-dextran (3TCSD) conjugate

The synthesis of 3TCSD conjugate was carried out in the laboratory of Dr. Keykavous Parang at the University of Rhode Island College of Pharmacy. The

complete procedure for the synthesis of 3TCSD conjugate is depicted in Schemes 1 and 2. The chemical structures of the intermediates and the final product were determined by nuclear magnetic resonance spectroscopy (^1H NMR) on a Bruker NMR spectrometer (400 MHz) and/or a high-resolution PE Biosystems Mariner API time-of-flight electrospray mass spectrometer.

2.3.1. (-)-5'-O-(tert-Butyldimethylsilyloxy)-2',3'-dideoxy-3'-thiacytidine (2)

tert-Butyl-dimethylsilyl chloride (TBDMSCl) (2.0 g, 13.27 mmol) and imidazole (360 mg, 5.29 mmol) were added to a solution of 3TC (**1**, 1.0 g, 4.36 mmol) in dry N,N-dimethylformamide (DMF) (50.0 mL). The reaction mixture was stirred at room temperature for 18 h. After completion of the reaction, the solvent was removed under reduced pressure, and the crude compound was purified by column chromatography over silica gel using hexane/dichloromethane as the eluents to afford **2** (1.47 g, 98%). ^1H NMR (400 MHz, CD_3OD , δ ppm): 8.21 (d, $J = 7.7$ Hz, 1H, H-6), 6.32 (dd, $J = 5.8$, $J = 2.8$ Hz, 1H, H-1'), 6.02 (d, $J = 7.7$ Hz, 1H, H-5), 5.26 (t, $J = 3.0$ Hz, 1H, H-4'), 4.18 (dd, $J = 11.8$, $J = 3.0$ Hz, 1H, H-5'), 3.96 (dd, $J = 11.8$, $J = 3.0$ Hz, 1H, H-5''), 3.54 (dd, $J = 12.5$, $J = 5.8$ Hz, 1H, H-2'), 3.19 (dd, $J = 12.5$, $J = 2.8$ Hz, 1H, H-2''), 0.95 (s, 9H, $\text{C}(\text{CH}_3)_3$), 0.15 (s, 6H, $\text{CH}_3\text{-Si}$); HR-MS (ESI-TOF) (m/z): $\text{C}_{14}\text{H}_{25}\text{N}_3\text{O}_3\text{SSi}$ calcd, 343.1386; found 344.3933 [$\text{M} + \text{H}^+$], 686.4590 [2M^+].

2.3.2. (-)-4-N-(4,4'-Dimethoxytrityl)-5'-O-(tert-butyl)dimethylsilyloxy)-2',3'-dideoxy-3'-thia-cytidine (3)

Compound **2** (1.0 g, 2.91 mmol) and 4,4'-dimethoxytrityl chloride (DMTrCl, 1.08 g, 3.19 mmol) were dissolved in dry pyridine (80 mL) and stirred for 4 h at 0 °C and then for additional 16 h at room temperature. The solution was then neutralized with aqueous sodium bicarbonate (5.0%) and extracted with dichloromethane (3 × 100 mL). The organic layer was dried with anhydrous sodium sulfate, and the solvent was removed under reduced pressure. The crude compound was purified by column chromatography over silica gel using hexane/dichloromethane containing 1.0% triethylamine as the eluents to yield **3** (1.79 g, 95%). ¹H NMR (400 MHz, CDCl₃, δ ppm): 7.81 (d, *J* = 7.7 Hz, 1H, H-6), 7.74 (dd, *J* = 5.7, *J* = 3.3 Hz, 1H, aromatic hydrogen, DMTr), 7.55 (dd, *J* = 5.7, *J* = 3.2 Hz, 1H, aromatic hydrogen, DMTr), 7.12-7.33 (m, 7H, aromatic hydrogens, DMTr), 6.82-6.88 (m, 4H, aromatic hydrogens, DMTr), 6.33 (dd, *J* = 5.2, *J* = 3.1 Hz, 1H, H-1'), 5.19 (t, *J* = 3.1 Hz, 1H, H-4'), 5.03 (d, *J* = 7.7 Hz, 1H, H-5), 4.30-4.45 (m, 1H, H-5'), 4.00-4.20 (m, 1H, H-5''), 3.81 (s, 6H, DMTr-OCH₃), 3.52 (dd, *J* = 12.2, *J* = 5.2 Hz, 1H, H-2'), 3.17 (dd, *J* = 12.2, *J* = 3.1 Hz, 1H, H-2''), 0.80 (s, 9H, C(CH₃)₃), 0.06 (s, 6H, CH₃-Si); HR-MS (ESI-TOF) (*m/z*): C₃₅H₄₃N₃O₅SSi calcd, 645.2693; found 686.4634 [M + K + 2H]⁺, 1289.3676 [2M - 1]⁺.

2.3.3. (-)-4-N-(4,4'-Dimethoxytrityl)-2',3'-dideoxy-3'-thiacytidine (4)

Compound **3** (1.10 g, 1.70 mmol) was stirred with 1 M solution of *tert*-butylammonium fluoride (TBAF) in THF (5.0 mL) in the presence of molecular

sieves (4Å) at room temperature for 12 h. The reaction mixture was concentrated under reduced pressure and dried under vacuum. The crude compound was purified by column chromatography over silica gel using hexane/dichloromethane containing 1.0% triethylamine as the eluents to yield **4** (0.89 g, 98%). ¹H NMR (CD₃OD, δ ppm): 8.53 (d, *J* = 7.8 Hz, 1H, H-6), 7.32-7.34 (m, 2H, aromatic hydrogens, DMTr), 7.17-7.23 (m, 6H, aromatic hydrogens, DMTr), 7.11-7.13 (m, 1H, aromatic hydrogen, DMTr), 6.75-7.78 (m, 4H, aromatic hydrogens, DMTr), 6.22 (dd, *J* = 5.3, *J* = 2.5 Hz, 1H, H-1'), 6.01 (d, *J* = 7.8 Hz, 1H, H-5), 5.25 (t, *J* = 3.1 Hz, 1H, H-4'), 3.99 (dd, *J* = 12.8, *J* = 3.1 Hz, 1H, H-5'), 3.84 (dd, *J* = 12.8, *J* = 3.1 Hz, 1H, H-5''), 3.69 (s, 6H, DMTr-OCH₃), 3.51 (dd, *J* = 12.6, *J* = 5.3 Hz, 1H, H-2'), 3.27 (dd, *J* = 12.6, *J* = 2.5 Hz, 1H, H-2''); HR-MS (ESI-TOF) (*m/z*): C₂₉H₂₉N₃O₅S calcd, 531.1828; found 531.9215 [M + H]⁺, 632.6915 [M + TEA]⁺.

2.3.4. (-)-4-N-(4,4'-Dimethoxytrityl)-5'-O-(succinate)-2',3'-dideoxy-3'-thiacytidine (5)

4-Dimethylaminopyridine (DMAP, 100 mg, 0.82 mmol) and succinic anhydride (290 mg, 2.90 mmol) were added to a solution of compound **4** (770 mg, 1.45 mmol) in dry pyridine (15.0 mL). The reaction mixture was stirred at room temperature overnight. After completion of the reaction, the solvent was evaporated under reduced pressure and the crude compound was purified by column chromatography over silica gel using dichloromethane/methanol containing 1% triethylamine as the eluents to yield **5** (0.82 g, 90%). ¹H NMR (400 MHz, DMSO-*d*₆, δ ppm): 8.56 (br s, 1H, NH), 7.60-7.70 (d, *J* = 7.8 Hz, 1H, H-6), 7.14-7.24 (m,

9H, aromatic hydrogens, DMTr), 6.72-6.84 (m, 4H, aromatic hydrogens, DMTr), 6.30-6.38 (m, 1H, H-1'), 6.10 (d, $J = 7.8$ Hz, 1H, H-5), 5.25-5.35 (m, 1H, H-4'), 4.22-4.34 (m, 2H, H-5' and H-5''), 3.71 (s, 6H, DMTr-OCH₃), 3.58-3.63 (m, 2H, H-2' and H-2''), 3.00-3.10 (m, 4H, CH₂CH₂); HR-MS (ESI-TOF) (m/z): C₃₃H₃₃N₃O₈S calcd, 631.1988; found 632.1715 [M + H]⁺, 654.1472 [M + Na]⁺.

2.3.5. (-)-5'-O-(Succinate)-2',3'-dideoxy-3'-thiacytidine (3TCS, 6)

Acetic acid (AcOH, 10 mL, 80%) was added to compound **5** (100 mg, 0.16 mmol). The reaction mixture was heated at 80 °C for 30 min. The solvent was removed under reduced pressure and the crude compound was purified by HPLC (acetonitrile/water gradient) to yield **6** (47 mg, 90%). ¹H NMR (400 MHz, DMSO-*d*₆, δ ppm): 12.29 (s, 1H, COOH), 9.50-9.80 (br s, 2H, NH₂), 7.60-7.70 (m, 1H, H-6), 6.20-6.32 (m, 1H, H-1'), 5.81-5.93 (m, 1H, H-5), 5.30-5.36 (m, 1H, H-4'), 4.30-4.40 (m, 2H, H-5' and H-5''), 3.71-3.80 (m, 2H, H-2'), 3.00-3.200 (m, 5H, H-2'' and CH₂CH₂); HR-MS (ESI-TOF) (m/z): C₁₂H₁₅N₃O₆S calcd, 329.0682; found 330.3316 [M + H]⁺, 658.3471 [2M]⁺.

2.3.6. (-)-Dextran-5'-O-(succinate)-2',3'-dideoxy-3'-thiacytidine (3TC-succinate-dextran conjugate, 3TCSD, 8)

DMAP (70.0 mg, 0.57 mmol), *N,N'*-diisopropylethylamine (DIPEA, 100 μL, 0.61 mmol), and *N,N'*-diisopropylcarbodiimide (DIC) (50 μL, 0.32 mmol) were added to a solution of compound **5** (275.0 mg, 0.44 mmol) and dextran 20 kDa (130 mg) in dry dimethylsulfoxide (DMSO, 3.0 mL) under nitrogen atmosphere. The reaction mixture was stirred at 40 °C for 48 h. After the completion of reaction, the

reaction mixture was cooled to room temperature and cold diethyl ether: ethanol (45 mL, 50:50 v/v) was added. The mixture was washed twice with cold ethanol: diethyl ether (50:50, v/v) and finally with cold ethanol: acetonitrile (70:30, v/v) and centrifuged. The precipitate was dried under vacuum to give (-)-dextran-4-*N*-(4,4'-dimethoxytrityl)-5'-*O*-(succinate)-2',3'-dideoxy-3'-thiacytidin [4-*N*-(4'-dimethoxytrityl)-lamivudine-dine-succinate-dextran conjugate, **7**].

Acetic acid (AcOH, 10 mL, 80%) was added to compound **6**. The reaction mixture was stirred at room temperature for 3 h and then heated at 80 °C for 30 min. The solvent was removed under reduced pressure and the residue was washed three times with cold diethyl ether: ethanol (45 mL, 50:50 v/v) and centrifuged to give 3TC-succinate-dextran conjugate (3TCSD, **8**). ¹H NMR (400 MHz, D₂O, δ ppm): 7.88-8.04 (br s, 1H, H-6), 6.25-6.35 (m, 1H, H-1'), 6.05-6.15 (br s, 1H, H-5), 5.41-5.50 (m, 1H, H-4'), 4.85-5.05 (m, anomeric hydrogen of dextran, H-1), 4.28-4.58 (m, 2H, H-5' and H-5''), 3.40-4.10 (m, H-2' and H-2'' of 3TC, H-2, H-3, H-4, H-5, and H6 of dextran), 3.30-3.38 (m, 4H, CH₂CH₂ of succinate).

2.4. Further characterization of 3TC-succinate-dextran conjugate (3TCSD, 8)

The purity of the powder was determined using both the size exclusion (SEC) and reversed-phase (RP) chromatographic methods. The degree of substitution of 3TC in 3TCSD was determined by hydrolysis of the conjugate under basic conditions. To 1 mg of the conjugate were added 1 ml of 0.1 N NaOH and 0.6 ml of methanol. After leaving at room temperature for 5 min, 30 min, and 24 h, 100

μl of the sample was micropipetted into a microcentrifuge tube containing 100 μl of 0.1 M HCl. An aliquot (50 μl) was then injected into HPLC. The concentration of the released 3TC was determined using a reversed-phase method based on 3TC standard solutions as described below.

2.5. High performance liquid chromatography

Size-exclusion (SEC) and reversed-phase (RPC) chromatographic methods were developed and validated for quantitation of the conjugate 3TCSD and its hydrolysis products (3TC and 3TCS), respectively, in buffers or biological samples.

2.5.1. Size-exclusion liquid chromatography (SEC)

Lamivudine-succinate-dextran conjugate (3TCSD) was analyzed in non-biological and biological (plasma and liver) samples at ambient temperature using a 30 cm x 7.8 mm analytical, gel chromatography column (PolySep-GFC 3000; Phenomenex, Torrance, CA). The mobile phase consisted of water: acetonitrile: acetic acid (75:25:0.2, v/v/v) and was pumped at a flow rate of 1.0 mL/min.

2.5.2. Reversed-phase liquid chromatography (RPC)

A reversed-phase chromatographic method was developed to quantitate the concentrations of 3TC and 3TCS in aqueous and biological samples. The separation of 3TC, 3TCS, and internal standard (stavudine, IS) was achieved on a 250 mm x 4.6 mm C18 column (Microsorb-MV, Varian, Lake Forest, CA) preceded by a 5-cm guard column. The mobile phase consisted of KH_2PO_4 (50 mM): methanol: triethylamine (90:10:0.1, v/v, pH 7.0), which was pumped at a flow rate of 1

mL/min.

2.5.3. HPLC system

The HPLC instrument consisted of a 510 pump (Waters; Milford, MA), a 717 plus auto sampler (Waters; Milford, MA), and a 486 UV detector (Waters) set at a wavelength of 276 nm. The chromatographic data was managed using Empower version 2 software. Calibration curves were constructed by plotting the peak areas of 3TCSD or peak area ratios of 3TC or 3TCS over IS against the concentration in the sample using a weight of 1/concentration.

2.5.4. Standard solutions

Stock solution of 3TCSD (0.5 mg/ml, 3TC equivalent) was prepared in water and diluted further with water or plasma to make final standard solutions of 0, 1, 2, 5, 10, 15, 25, and 50 µg/ml (3TC equivalent). Stock solution of 3TC (1 mg/ml) was prepared in water and kept at -20 °C, whereas the stock solution of 3TCS (1 mg/ml; 3TC equivalent) was prepared in methanol and stored at -20 °C. The standards of 3TC (0.125, 0.25, 0.5, 1.0, 2.0, 5.0, 10, and 20 µg/ml) and 3TCS (0, 0.36, 0.72, 1.80, 3.6, 5.4, 9.0, and 18 µg/ml, 3TC equivalent) were prepared daily by diluting the stock solution with water or blank plasma for quantitation of analytes in aqueous and plasma samples, respectively.

2.5.5. Sample preparation

For the size exclusion chromatography, to 100 µl of plasma in microcentrifuge tubes were added 20 µl of methanol and 20 µl of 20% (w/v)

trichloroacetic acid. After vortex mixing for 5 s, the samples were centrifuged in a microcentrifuge at 16,000 rpm for 5 min. A 100 μ l aliquot of the supernatant was mixed with 50 μ l of 0.5 M phosphate buffer (pH 7.0), and a 75- μ l aliquot was injected into the HPLC.

To determine the concentrations of 3TCSD in the tissues by the SEC method, tissues were homogenized in 3 volumes of water using a homogenizer at a rate of 10,000 rpm. To 100 μ l of the whole homogenate in siliconized microcentrifuge tubes were added 50 μ l of 0.5 M phosphate buffer (pH 7.0) and 50 μ l of methanol. Samples were then briefly vortex-mixed and 40 μ l of trichloroacetic acid (40 %) was added to precipitate proteins. After vortex-mixing for 5 s, the samples were centrifuged in a microcentrifuge at 10,000 rpm for 3 min. A 100 μ l aliquot of the supernatant was mixed with 50 μ l of 1 M sodium acetate, and a 75- μ l aliquot was injected into the HPLC.

The preparation of plasma samples for reversed-phase chromatography was similar to that for the SEC method with one exception; for the reversed-phase system, 50 μ l of 50 μ g/ml stavudine was added as internal standard to the plasma sample before protein precipitation. Similarly, the tissue samples for reversed-phase chromatography were prepared as described above for the SEC method, but without the addition of 0.5 M phosphate buffer.

Analysis for urine samples for both reversed phase and size-exclusion chromatography was similar to that in plasma.

2.5.6. Validation of assays

The inter-run precision (%CV) and accuracy (%error) of the assays were determined from the analysis of quality control samples ($n=5$) based on reported guidelines (Shah et al., 1992). The concentrations of quality control samples were 1.0, 10, or 50 $\mu\text{g/ml}$ for 3TCSD (SEC method), 0.125, 5.0, and 20 $\mu\text{g/ml}$ for 3TC (RPC method), and 0.36, 5.4, and 18 $\mu\text{g/ml}$ for 3TCS (RPC method).

2.5.7 Recovery

To determine the recovery of 3TCSD, 3TC, and 3TCS from plasma after protein precipitation, plasma samples ($n=5$) containing 5 or 100 $\mu\text{g/ml}$ 3TCSD, 5 or 50 $\mu\text{g/ml}$ 3TC, or 1.8 or 18 $\mu\text{g/ml}$ 3TCS were subjected to the above assays and the peak areas were determined. The peak areas of these samples were then compared with those containing an equal concentration of each analyte in distilled water, injected directly into the HPLC. Similarly, the recoveries of 3TCSD and 3TC from the liver samples ($n=5$) containing 5 $\mu\text{g/ml}$ 3TCSD or 0.5 $\mu\text{g/ml}$ of 3TC were determined.

2.6. In vitro release characteristic

2.6.1. Release characteristics in buffers

The prodrug (3TCSD), at a concentration equivalent to 100 $\mu\text{g/ml}$ 3TC, was dissolved in 10 mM KH_2PO_4 (pH 4.4) or phosphate buffer (pH 7.4). The solutions were then incubated at 37 $^\circ\text{C}$ ($n=3$). Samples (100 μl) were taken at 0, 3, 6, 12, and

24 h and subjected to the above HPLC methods for the quantitation of intact 3TCSD (SEC method) and released 3TC or 3TCS (RP method).

2.6.2. Release characteristics in rat blood

Blood was obtained from adult male Sprague-Dawley rats by cardiac puncture. Approximately 4 IU of heparin was added to each ml of blood to prevent coagulation. Immediately after the collection of blood, 3TCSD conjugate (in 10 mM isotonic phosphate buffer at pH 7.4) was added to produce a blood concentration of 100 µg/ml (3TC equivalent) ($n=3$). The solution was then incubated at 37 °C. Blood samples (1 ml) were collected at 0, 3, 6, and 12 h in heparinized microcentrifuge tubes. After centrifugation of the blood, the plasma samples (100 µl) were subjected to the assays described above for the determination of 3TC, 3TCS, and/or intact 3TCSD.

2.6.3. Release characteristics in rat liver lysosomes

Crude lysosomal fractions were prepared from the liver of untreated rats according to the procedure described in the lysosome isolation kit (Sigma). Briefly, the rat livers were perfused with ice-cold PBS before removal of the livers. The livers were then homogenized in 4 volumes of the extraction buffer, followed by differential centrifugation for isolating the lysosomal fraction. The protein concentrations in lysosomal preparations were determined by Bio-Rad protein assay (Bio-Rad, Hercules, CA, USA). The activity of acid phosphatase, a lysosomal marker, in the preparation was tested using a commercial kit (Sigma). The specific

enzyme activity in the lysosomal fraction was >9-fold that in the liver homogenate.

For lysosomal hydrolysis studies, 3TCSD (100 µg/mL, 3TC equivalent) was incubated at 37 °C in 50 mM acetate buffer (pH 4.0) in the presence of 5 mM reduced glutathione and 5 mg/mL lysosomal protein ($n = 3$). Control samples were prepared in the absence of lysosomal proteins. Samples (100 µL) were then taken at 0, 3, 6, 9, 12, and 24 h and treated as described above before reversed-phase and size-exclusion HPLC analysis.

2.7. In vivo disposition

A total of 42 adult male Sprague-Dawley rats were divided equally into two groups of 21 rats each, treated with 3TCSD or 3TC. The mean \pm S.D. of the body weights of rats were 241 ± 8 and 240 ± 6 g for the 3TCSD- and 3TC-injected groups, respectively. The animals had free access to drinking water and rat chow before and during the course of experiments.

Single iv bolus doses (5 mg/kg; 3TC equivalent) of 3TCSD or the parent drug 3TC were injected into the penile vein of the animals under isoflurane anesthesia. Different groups of rats ($n = 3$ /group/time point) were euthanized at 0 (before drug administration), 5, 15, 60, 120, or 180 min following drug administration, and liver and blood (cardiac puncture) were collected. Additionally, total urine output was collected from zero to 180 min or to 24 h for the 3TC- or 3TCSD-injected group ($n = 3$ /group) by keeping the rats in metabolism cages.

Immediately after excision, the liver was rinsed in ice-cold saline solution to remove excess blood. Afterwards, the livers were blotted dry and kept frozen until

analysis. After centrifugation of the blood in a pre-chilled and heparin-coated microcentrifuge tube, the plasma was collected. To prevent in vitro hydrolysis of 3TCSD during storage, plasma (500 μL) was mixed with a 10% acetic acid solution (100 μL). Plasma, liver, and urine samples were kept frozen at $-80\text{ }^{\circ}\text{C}$ until analysis.

2.8. Pharmacokinetic analysis

Non-compartmental analysis was performed by using WinNonlin™ 5.0.1 computer program (Pharsight Co.; Mount View, California). Terminal elimination rate constant (λ_z) was estimated from the log-linear portion of the plasma or tissue concentration-time courses. Area under the plasma or tissue concentration-time curve (AUC) was estimated from the average plasma or tissue concentrations at different time points using linear trapezoidal rule with extrapolation to infinity only for the plasma profiles. For tissues, AUCs were not extrapolated beyond the quantifiable samples because of uncertainty about the terminal half lives. Other estimated pharmacokinetic parameters included: apparent total body clearance (CL), renal clearance (CL_R), volume of distribution at steady-state (V_{ss}), terminal volume of distribution (V_z), fraction of the drug excreted unchanged in urine (f_e), mean residence time (MRT), and maximum observed drug concentration (C_{max}). The maximum concentrations of 3TCSD or 3TC in plasma (C_0) after the injection of the conjugate or parent drug were estimated by the program. The concentrations of drugs in tissues were corrected for the residual blood using the volume fraction of different tissues (Mehvar et al., 1994).

2.9. Statistical analysis

Because of destructive sampling procedure used for the collection of blood and liver from different animals at each time point, the composite kinetic parameter AUC could not be obtained for individual rats (Mehvar et al., 1994). Therefore the variance of AUC was estimated by a reported (Bailer, 1988; Yuan, 1993), procedure based on the standard error of mean and number of samples at each time point. The pairwise comparison of AUCs was then carried out at an α level of 0.05 and a Bonferroni-adjusted α of 0.05 or 0.0167 for pairwise comparison of two (1 comparison) or three (3 comparison) means, respectively. The critical values of Z (Z_{crit}) for the two-sided test using the Bonferroni-adjusted α of 0.05 and 0.0167 were 1.96 and 2.39, respectively, and the observed Z (Z_{obs}) was calculated as reported before (Bailer, 1988; Yuan, 1993). A Z_{obs} value $> Z_{crit}$ was used as an indication of a significant difference between the AUCs.

The differences between groups in their kinetic parameters that could be estimated for individual rats (e.g., C_{max} and CL_R) were determined using a two-tailed unpaired t test at a significance level (α) of 0.05. When possible, data are presented as mean \pm S.D.

CHAPTER III

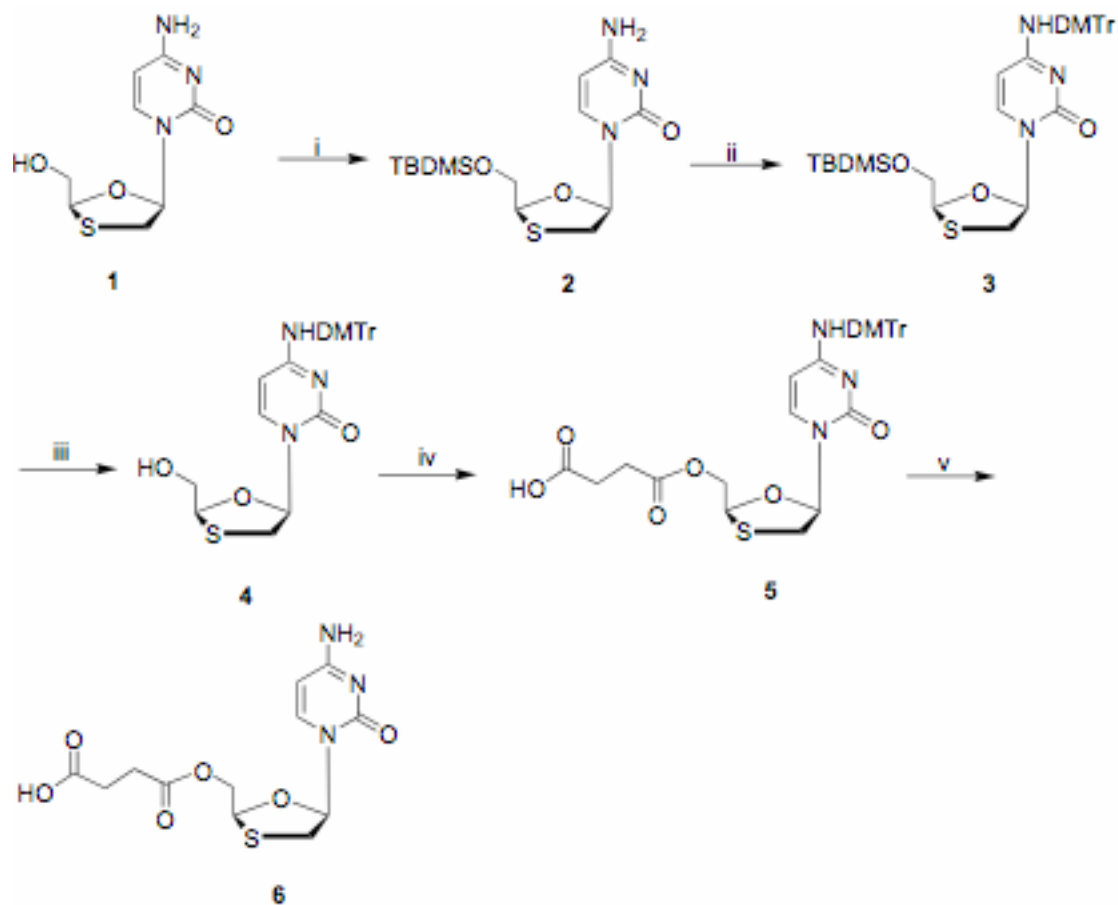
RESULTS

3.1. Synthesis and characterization of 3TCSD

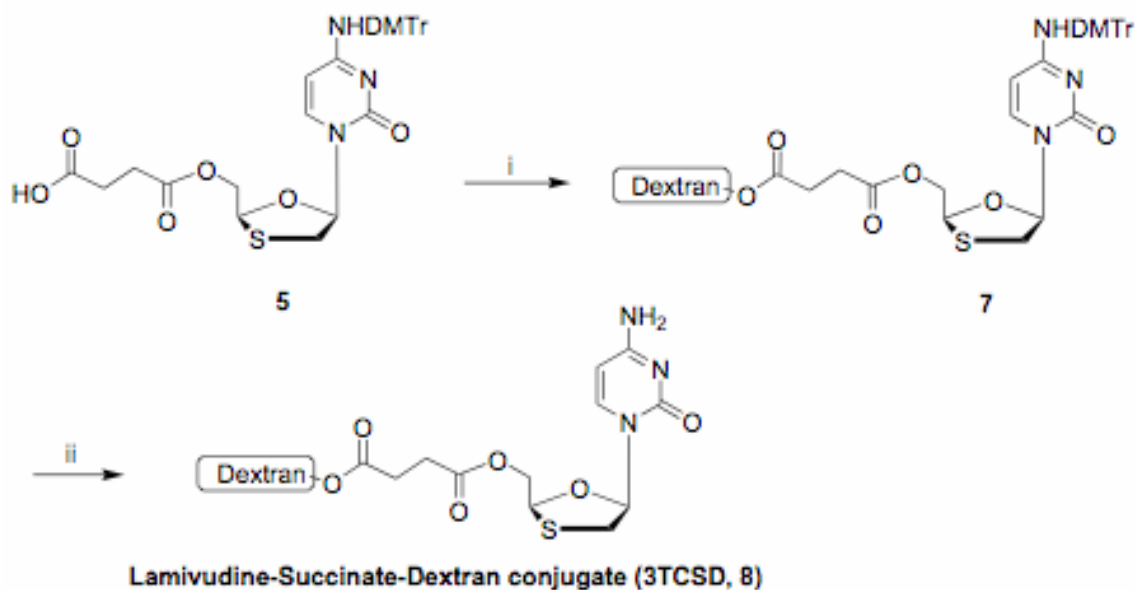
Lamivudine (3TC) was conjugated to dextran using a succinate linker in two major steps by synthesis of 5'-*O*-succinate ester of the drug (Scheme 2), followed by the reaction of the ester conjugate with dextran (Scheme 3). Lamivudine was initially reacted with TBDMSCl in the presence of imidazole to yield 5'-*O*-TBDMS-lamivudine (**2**). The protection of *N*4-amino group of 5'-*O*-protected lamivudine was carried out in the presence of DMTr-Cl and pyridine to give *N*4-DMTr-5'-*O*-TBDMS-lamivudine (**3**). The deprotection of 5'-*O*-TBDMS in the presence of tetrabutylammonium fluoride afforded *N*4-DMTr derivative of lamivudine (**4**), which was used in the reaction with succinic anhydride to generate *N*4-DMTr-5'-*O*-succinate ester conjugate of lamivudine (**5**) (Scheme 2). Compound **5** was reacted with dextran in the presence of DIC and DMAP to afford *N*4-(DMTr)lamivudine-succinate-dextran conjugate (**7**) that was deprotected in the presence of acetic acid to afford lamivudine-succinate-dextran conjugate (3TCSD, **8**) (Scheme 3).

The purity of the conjugate was >99% as determined by the reversed phase analysis of a 100- μ g/ml solution of the conjugate ($n = 3$), which contained only 0.296 ± 0.041 μ g/ml of 3TC without any measurable peak of 3TCS. The degree of

substitution of our final product, which was obtained by the base hydrolysis of 3TCSD to 3TC followed by reversed-phase quantitation of the released 3TC, was 6.5 mg lamivudine in 100 mg of 3TCSD powder. The complete hydrolysis of 3TCSD was confirmed by a complete disappearance of the 3TCSD peak in the SEC method. Additionally, the area of the unhydrolyzed 3TCSD peak in the SEC method was the same as the area of the released 3TC peak in the reversed-phase method after appropriate volume correction, indicating that the degree of substitution may be determined directly from the area of 3TCSD peak without hydrolysis.



Scheme 2: Synthesis of 4-*N*-(4,4'-dimethoxytrityl)-5'-*O*-(succinate)-2',3'-dideoxy-3'-thiacytidine (4-*N*-(4,4'-dimethoxytrityl)lamivudine succinate, 5). Reagents: (i) TBDMSCl, imidazole, DMF; (ii) DMTrCl, pyridine; (iii) TBAF, molecular sieves (4Å); (iv) succinic anhydride, DMF, pyridine, DMAP; (v) AcOH (80%).



Scheme 3: Synthesis of 3TC-succinate-dextran (3TCSD, 8). Reagents: (i) dextran 25 kDa, DIC, DMAP, DMSO, DIPEA; (ii) AcOH (80%).

3.2. Size-exclusion chromatographic method

Chromatograms of plasma samples taken from a rat before (blank) and 180 min after the administration of a single 5-mg/kg dose (3TC equivalent) of 3TCSD are demonstrated in Fig. 1. Dextran-lamivudine succinate eluted at ~5.3 min and was well separated from the endogenous peaks in plasma, which eluted after the conjugate peak (Fig. 1). Additionally, the relationship between the peak area of 3TCSD and the detector response was linear ($r^2 \geq 0.998$) over the studied range 1 to 50 $\mu\text{g/mL}$.

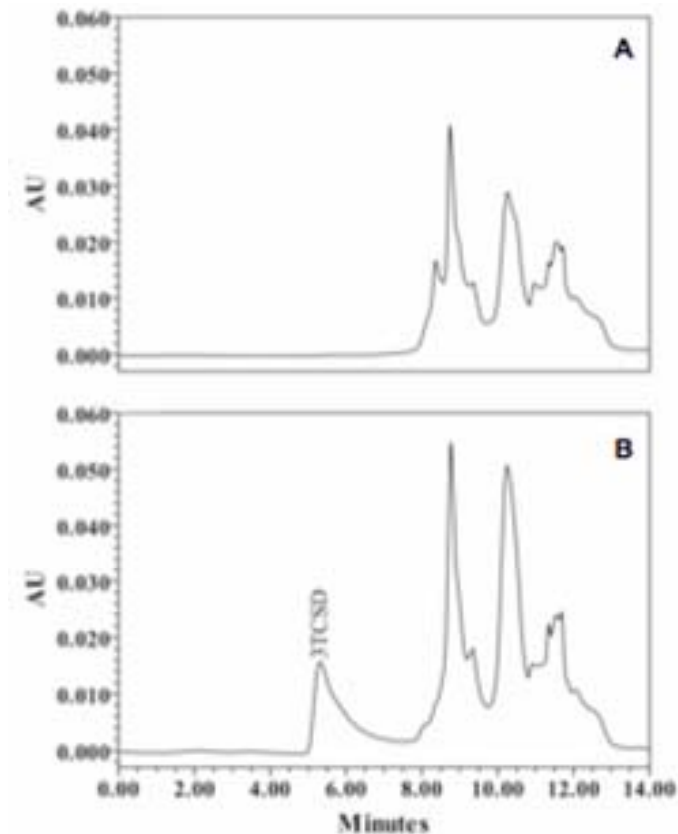


Figure 1: Chromatograms of plasma samples taken from a rat before (A) and 180 min after (B) the administration of a single 5-mg/kg dose (3TC equivalent) of 3TCSD, subjected to the size-exclusion chromatographic method. The 180-min sample contained 9.70 $\mu\text{g/mL}$ of 3TCSD.

Table 2 lists the response of the detector to various concentrations of 3TCSD in the sample for 5 different calibration curves. The relationship between the peak area of 3TCSD and the detector response was linear ($r^2 \geq 0.998$, Table 2) over the studied range of 1 to 100 $\mu\text{g/mL}$. Additionally, the variability in the slopes (C.V.) was relatively low (9.23%).

Table 2: Relationship between the 3TCSD peak area and the added plasma concentration [Peak area=Intercept + (slope x Conc)] for the SEC method

Calibration #	Intercept	Slope	R ²
1	11200	93400	0.999
2	21000	83700	0.999
3	8010	83300	0.999
4	1490	79800	0.999
5	25000	72300	0.998

The results of the assay validation for the inter-run experiments are presented in Table 3. Excellent accuracy of the assay is demonstrated by error values of <1% for all the concentrations (even at the lowest concentration of 1 µg/ml). The assay is also deemed precise because the C.V. values are <13% for the inter-run data (Table 3). Based on the data presented in Table 3, the limit of quantitation of the assay is at least equal to 1 µg/ml.

Table 3: Inter-run accuracy and precision for quantitation of 3TCSD using the SEC assay (n = 5)

Added Conc. (µg/ml)	Calculated Conc. (µg/ml)	CV (%)	Error (%)
1	0.992	12.8	-0.84
10	10.1	2.34	0.70
50	49.6	1.60	-0.80

The recovery of 3TCSD from plasma was $88.0 \pm 4.2\%$ and $94.1 \pm 4.6\%$ at concentrations of 5 and 50 µg/ml, respectively. The recovery of 3TCSD from liver was $94.2 \pm 9.5\%$ at a concentration of 5 µg/ml.

3.3. Reversed-phase chromatographic method

Figure 2 depicts the chromatograms of plasma samples at zero (blank) and 15 min after the administration of a single 5-mg/kg dose of 3TC to rats and at 3 h after the in vitro incubation of 3TCSD in blood. Lamivudine, internal standard (stavudine), and 3TCS eluted at ~11, 17, and 26 min, respectively and were well separated from the endogenous peaks in plasma (Fig. 2). Additionally, the relationship between the peak area ratios of 3TC and 3TCS and the sample concentrations was linear ($r^2 \geq 0.998$) over the studied concentration range of 0.125 to 20 $\mu\text{g/mL}$ for 3TC and 0.36 to 18 $\mu\text{g/mL}$ (3TC equivalent) for 3TCS.

Table 4 lists the characteristics of five inter-run calibration curves for 3TC and 3TCS in plasma samples. The relationship between the peak area ratios of 3TC and 3TCS and the sample concentrations was linear ($r^2 \geq 0.998$) over the studied concentration range of 0.125 to 20 $\mu\text{g/ml}$ for 3TC and 0.36 to 18 $\mu\text{g/ml}$ (3TC equivalent) for 3TCS. Additionally, the degrees of variability (C.V.) in the slopes of inter-run calibrations were 12% and 11% for 3TC and 3TCS, respectively.

Validation results for the reversed-phase assay of 3TC and 3TCS are presented in Table 5. Excellent accuracy of the assay is demonstrated by error values of <11% for all the concentrations. The assay is also deemed precise because the C.V. values are <9% for all the concentrations except for the the lowest concentration of 3TC, which showed an acceptable C.V. of 16.8% (Table 5). Based on the data presented in Table 5, the limit of quantitation of the assay is 0.125 and 0.36 $\mu\text{g/ml}$ for 3TC and 3TCS, respectively.

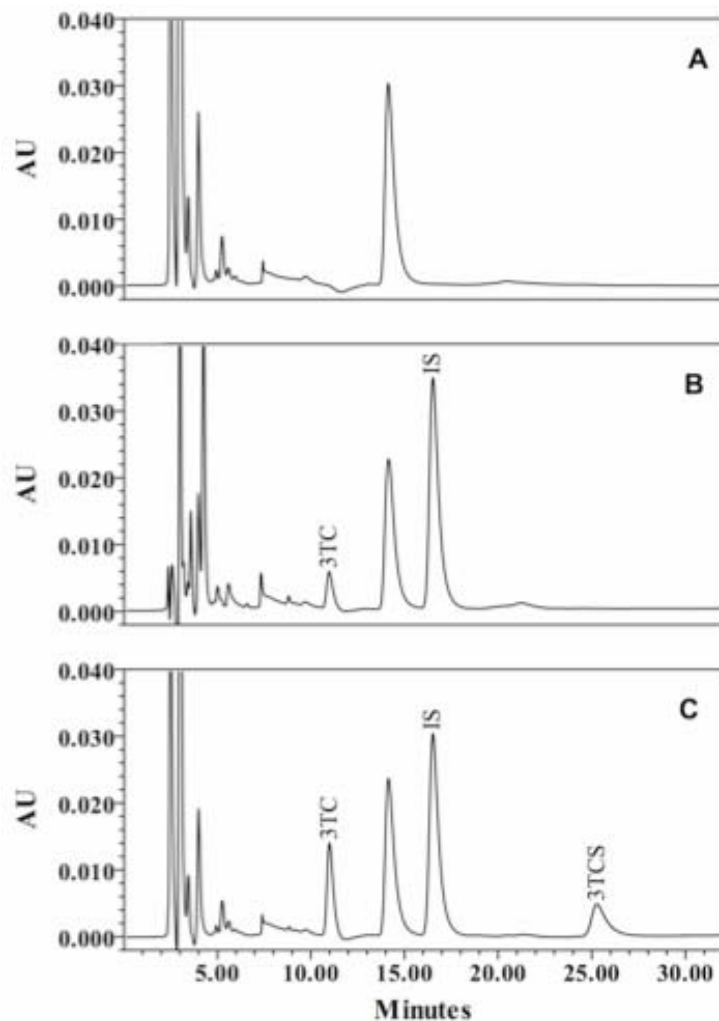


Figure 2: Chromatograms of plasma samples taken from a rat before (A) and 15 min after (B) the administration of a single 5-mg/kg dose of 3TC to rats and at 3 h after in vitro incubation of 3TCSD with rat blood (C), subjected to the reversed-phase chromatographic method. Sample B contained 1.84 $\mu\text{g/mL}$ of 3TC and sample C contained 3.97 and 5.12 $\mu\text{g/mL}$ of 3TC and 3TCS, respectively.

Table 4: Relationship between analyte: internal standard peak area ratio and the added plasma concentration [Peak area=Intercept + (slope x Conc.)] for reversed-phase method

Analyte	Calibration #	Intercept	Slope	R^2
3TC	1	-0.107	3.03	0.995
	2	-0.217	3.05	0.999
	3	-0.157	2.98	0.999
	4	-0.168	3.10	0.997
	5	-0.135	3.24	0.998
3TCS	1	-0.423	2.86	0.999
	2	-0.307	2.47	0.999
	3	-0.307	2.97	0.999
	4	-0.393	2.30	0.999
	5	-0.546	2.83	0.983

Table 5: Inter-run accuracy and precision for quantitation of 3TC and 3TCS in plasma using the reversed-phase assay ($n = 5$)

Analyte	Added Conc. ($\mu\text{g/ml}$)	Calculated Conc. ($\mu\text{g/ml}$)	CV (%)	Error (%)
3TC	0.125	0.138	16.8	10.9
3TC	5.0	4.75	3.15	-5.04
3TC	20	20.8	5.83	4.00
3TCS	0.36	0.378	8.33	5.14
3TCS	5.4	5.18	4.18	-3.73
3TCS	18	18.8	3.93	4.32

For 3TC, the degrees of recovery from plasma were $101 \pm 1.8\%$ and $104 \pm 1.8\%$ at concentrations of 5 and 50 $\mu\text{g/ml}$, respectively. For 3TCS, the values were 89.7 ± 8.5 and 85.7 ± 2.6 at concentrations of 1.8 and 18 $\mu\text{g/ml}$, respectively. The recovery of 3TC from the liver samples at a concentration of 0.5 $\mu\text{g/ml}$ was $95.7 \pm 5.25\%$.

3.4. Release characteristics in buffers

The SEC and reversed-phase HPLC assays described above were used to investigate the stability of 3TCSD and formation of 3TC and 3TCS at 37 °C at pH 4.4 (Fig. 3) or 7.4 (Fig. 4). The conjugate was very stable at pH 4.4 as demonstrated by both SEC (Fig. 3, top) and reversed-phase (Fig. 3, bottom) assays. The concentrations of 3TCSD did not significantly change over 24 h of incubation at 37 °C at pH 4.4 (Fig. 3, top). Additionally, reversed-phase analysis showed minor concentrations (< 1% of the initial concentration of 3TCSD) of 3TC and 3TCS released over the incubation time of 24 h (Fig. 3, bottom). On the other hand, measurable hydrolysis of 3TCSD occurred at pH 7.4 (Fig. 4). In the SEC method, the concentrations of 3TCSD declined ~ 16% during 24 h of incubation at pH 7.4 and 37 °C, with an apparent first-order half life of 108 h (Fig 4, top). The decline in the concentration of 3TCSD (Fig. 4, top) was associated with an almost identical increase in the concentrations of free 3TC and 3TCS in the sample analyzed by the reversed-phase method (Fig 4, bottom).

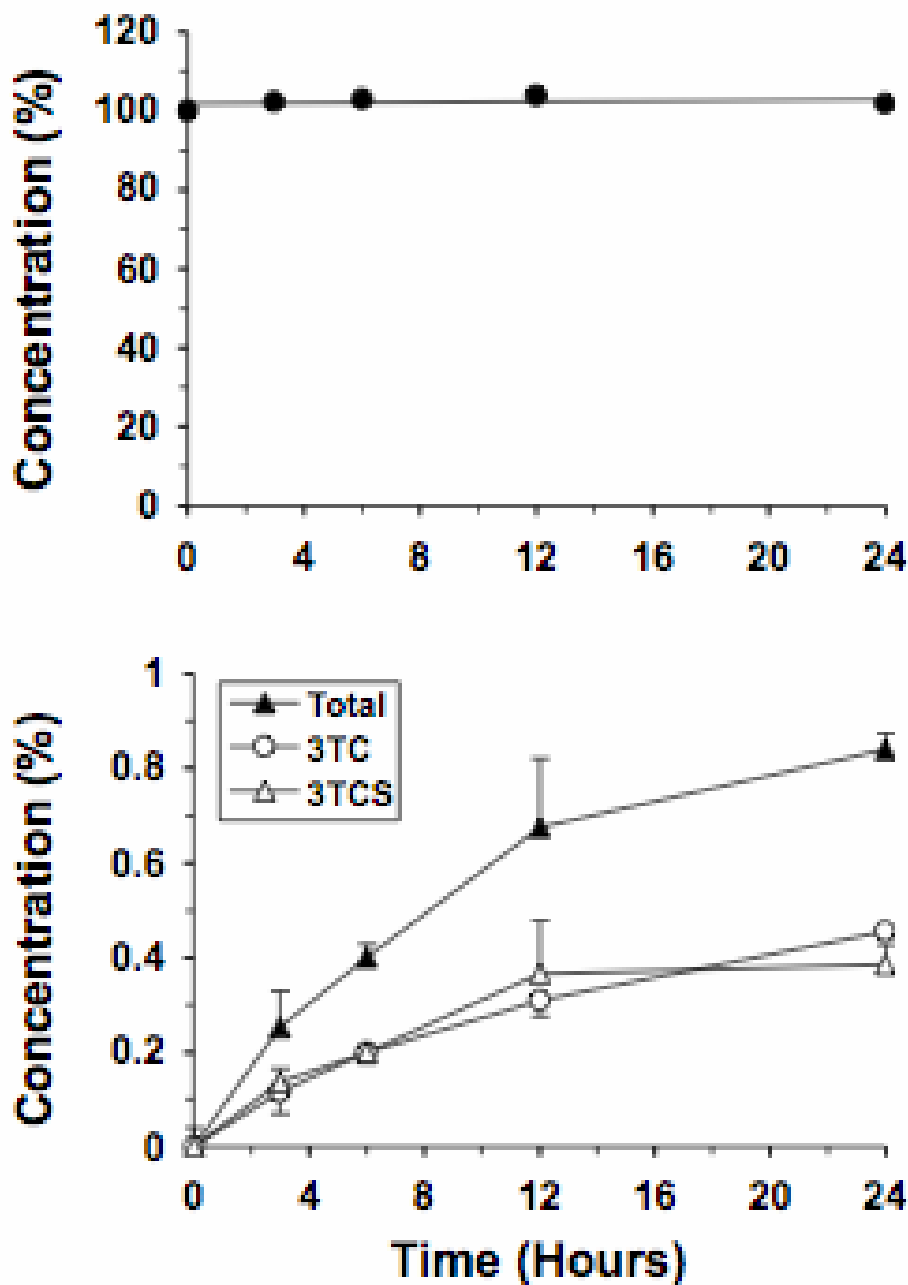


Figure 3: Average concentration-time courses of the intact 3TCSD (top) and released 3TC, 3TCS, and total 3TC (3TC plus 3TCS) (bottom) after incubation of the conjugate at pH 4.4 (37 °C). Error bars represent S.D. values ($n = 3$). Error bars for 3TCSD are too small to be observable.

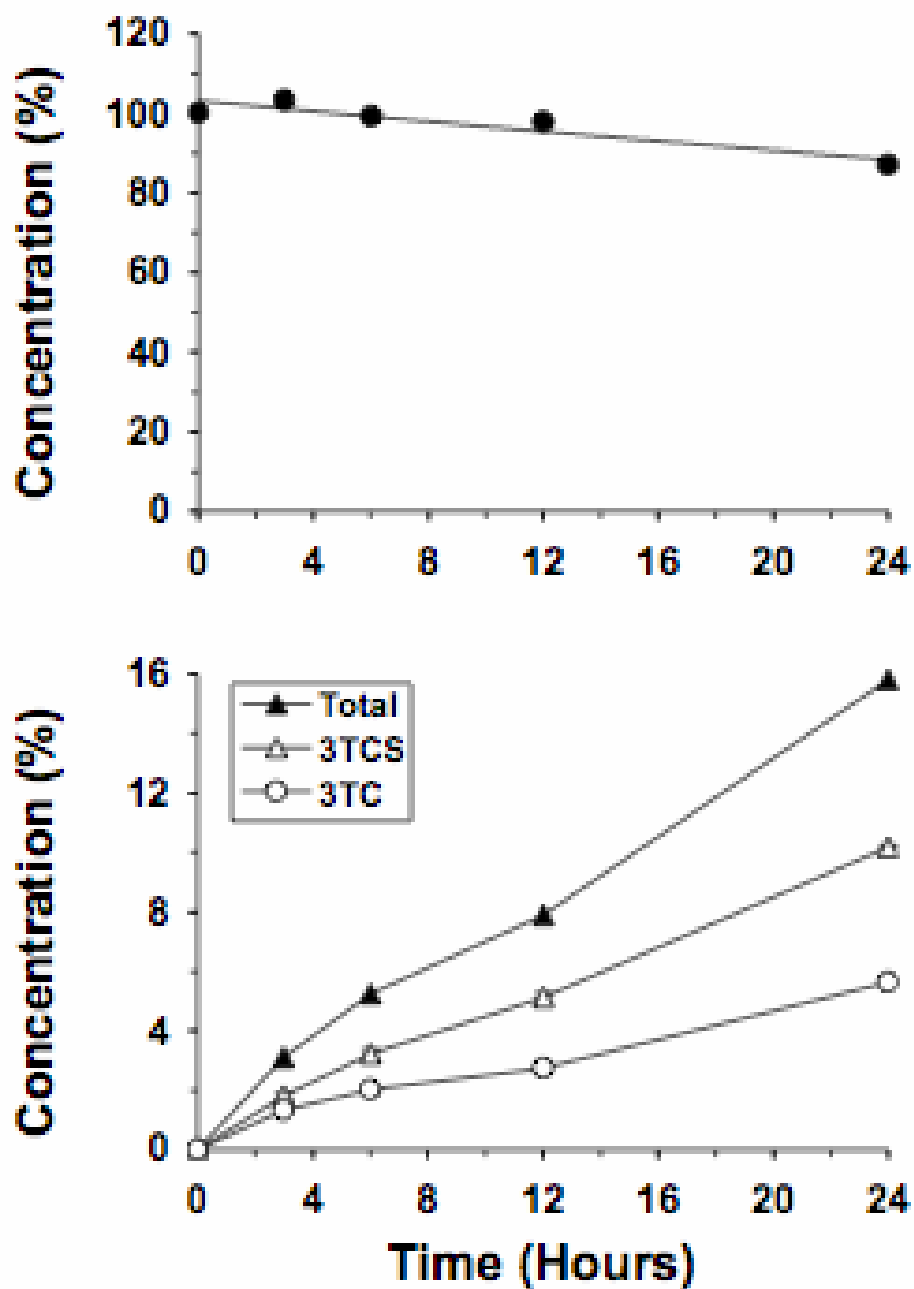


Figure 4: Average concentration-time courses of the intact 3TCSD (top) and released 3TC, 3TCS, and total 3TC (3TC plus 3TCS) (bottom) after incubation of the conjugate at pH 7.4 (37 °C). Error bars represent S.D. values ($n = 3$). In most cases, error bars are too small to be observable.

3.5. Release characteristics in rat blood

Figure 5 shows the decline in the 3TCSD concentration (top) and associated increases in the concentrations of 3TC and 3TCS (bottom), after incubation of the conjugate in rat blood at 37 °C. The total 3TC (3TC plus 3TC succinate) released during 12 h of incubation in blood was $8.45 \pm 0.04\%$ (Fig. 5, bottom) in agreement with an equivalent decline ($7.75 \pm 0.80\%$) in the concentration of the prodrug in the SEC assay (Fig. 5, top). The first-order half life of the decline in the 3TCSD concentration in plasma was 110 h.

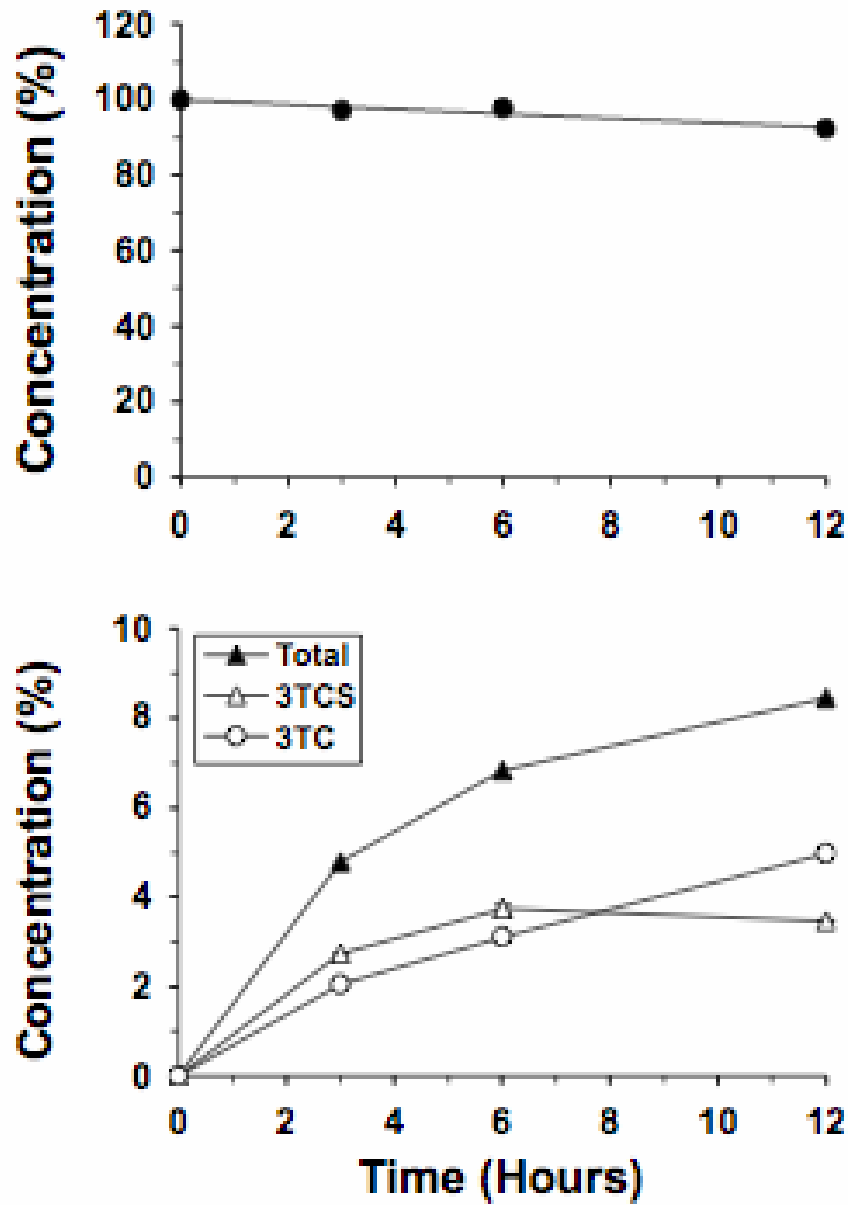


Figure 5: Average concentration-time courses of the intact 3TCSD (top) and released 3TC, 3TCS, and total 3TC (3TC plus 3TCS) (bottom) after incubation of the conjugate in rat blood (37 °C). Error bars represent S.D. values ($n = 3$). In most cases, error bars are too small to be observable.

3.6. Release characteristics in rat liver lysosomes

The concentration-time courses of 3TC release following incubation of 3TCSD in the presence and absence of rat liver lysosomes are depicted in Fig. 6. Presence of lysosomes in the medium induced a slow release of 3TC (7.36 ± 0.30 $\mu\text{g}/\text{mL}$ after 24 h) without any detectable 3TCS. In contrast, the release of 3TC or 3TCS in the same medium in the absence of lysosomes was negligible (Fig. 6).

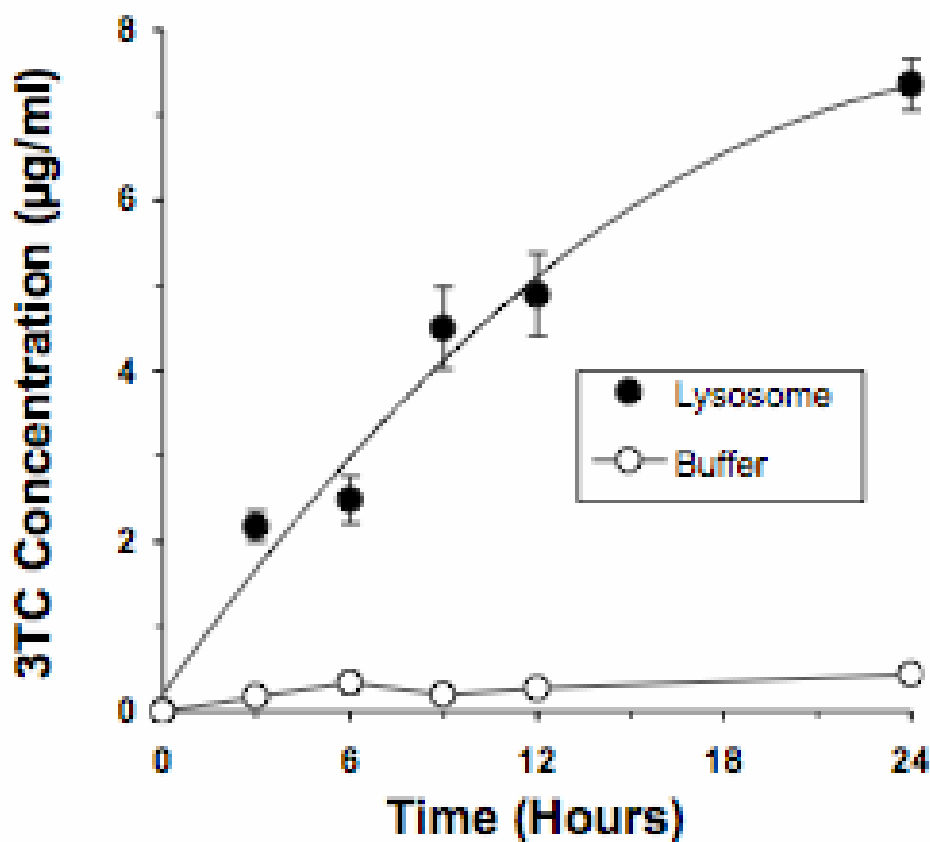


Figure 6: Average concentration-time courses of released 3TC after incubation of the conjugate in rat liver lysosomes or buffer (37 °C) at pH 4.0. Error bars represent S.D. values ($n = 3$). In most cases, error bars are too small to be observable.

3.7. In vivo disposition

Plasma concentration-time courses of 3TCSD and 3TC after the injection of single 5-mg/kg (3TC equivalent) doses of the prodrug or the parent drug are depicted in Fig. 7. After the injection of unconjugated 3TC, the drug was eliminated relatively rapidly and could not be detected at the last sampling time of 3 h (Fig. 7). In contrast, the concentrations of 3TCSD were several fold higher than those of 3TC and remained high even at the last sampling time after the injection of the conjugate. The plasma concentrations of both 3TC and 3TCSD declined multi-exponentially (Fig. 7). Additionally, no quantifiable concentrations of 3TC or 3TCS were detected in plasma of 3TCSD-injected rats.

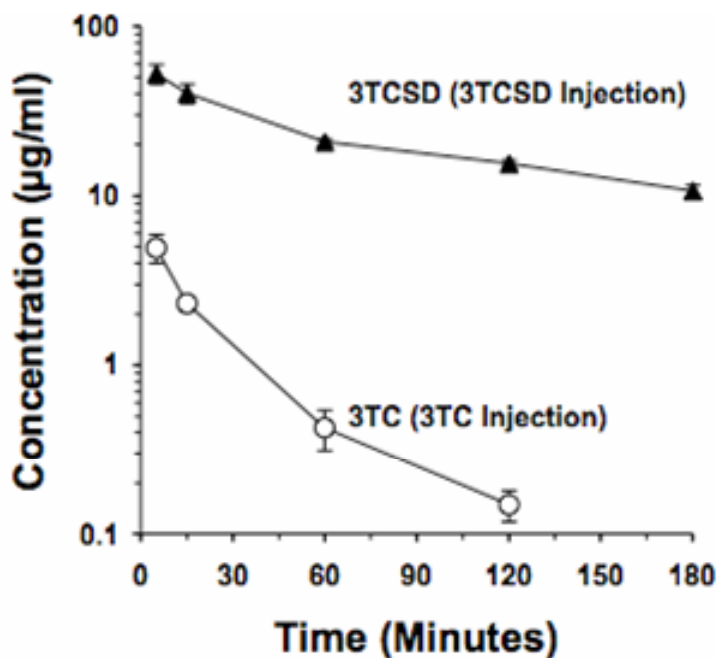


Figure 7: Plasma concentration-time courses of the conjugated (3TCSD) and unconjugated (3TC) lamivudine after iv administration of single, 5-mg/kg doses (3TC equivalent) of 3TC or 3TCSD to rats. Standard deviation values are shown as error bars ($n = 3$ rats for each point).

The plasma pharmacokinetic parameters of 3TC and 3TCSD after the injection of the parent drug or the prodrug are listed in Table 6.

Table 6: Plasma Pharmacokinetic Parameters (Mean \pm S.D.) of Unconjugated (3TC) and Dextran-Conjugated (3TCSD) Lamivudine after a Single iv Dose (5 mg/kg, 3TC Equivalent) of 3TC or 3TCSD

Parameter	3TC-Injected Rats	3TCSD-Injected Rats ^a
	3TC	3TCSD
C_{max}, $\mu\text{g/mL}$	4.94 \pm 0.93 [†]	52.5 \pm 6.5
AUC, $\mu\text{g min/mL}$	153 \pm 7 [†]	5930 \pm 153
CL, mL/min per kg	32.6 ^b	0.844 ^b
CL_R, mL/min per kg	21.3 \pm 2.1 [†]	0.263 \pm 0.089
f_e, %	65.3 \pm 6.5 [†]	31.2 \pm 10.6
V_z, mL/kg	1786 ^b	152 ^b
V_{ss}, mL/kg	930 ^b	135 ^b
λ_z, min⁻¹	0.0183 ^b	0.00554 ^b
t_{1/2}(λ_z), min	37.9 ^b	125 ^b
MRT, min	28.5 ^b	160 ^b

^a No quantifiable concentrations of 3TC or 3TCS were detected in plasma after 3TCSD injection.

^b Standard deviations could not be determined because of destructive sampling method.

[†] Significantly different ($P < 0.05$) from the corresponding value for the 3TCSD-injected rats.

Conjugation of 3TC to dextran resulted in an almost forty-fold decrease in the total CL of the drug and a similar degree of increase in its plasma AUC. The decrease in total CL was associated with an eighty-fold decrease in the CL_R of the drug when conjugated to dextran. Consequently, the fraction of the drug excreted unchanged into urine decreased from 65% for the parent drug to 31% for the conjugate (Table 6). Additionally, dextran conjugation decreased the extent of distribution of the drug as reflected in V_{ss} and V_z values (Table 5), although to a lesser degree than that seen with the CL values (7-12 fold versus 40-80 fold, respectively). The declines in both the clearance and volume of distribution upon conjugation resulted in longer terminal half life and MRT values for the conjugate, compared with the parent drug (Table 6).

The hepatic concentration-time courses (top) and AUC values (bottom) of the conjugate and regenerated 3TC after the administration of the conjugate and those of 3TC after the injection of the parent drug itself are depicted in Fig. 8. After the injection of 3TC, the hepatic concentrations of the drug were measurable only in the first two samples; no detectable 3TC levels were found in the liver beyond 15 min following the administration of the parent drug (Fig. 8, top). However, relatively high concentrations of 3TCSD were detected until the last sampling point. This resulted in > fifty-fold higher ($P < 0.0001$) AUCs for the conjugated 3TC, compared with the parent drug (Fig. 8, bottom). Additionally, the conjugated 3TC slowly released 3TC in the liver (Fig. 8, top) with an AUC that was approximately

2.5-fold larger ($P < 0.0001$) than that of the parent drug during the sampling time (Fig. 8, bottom).

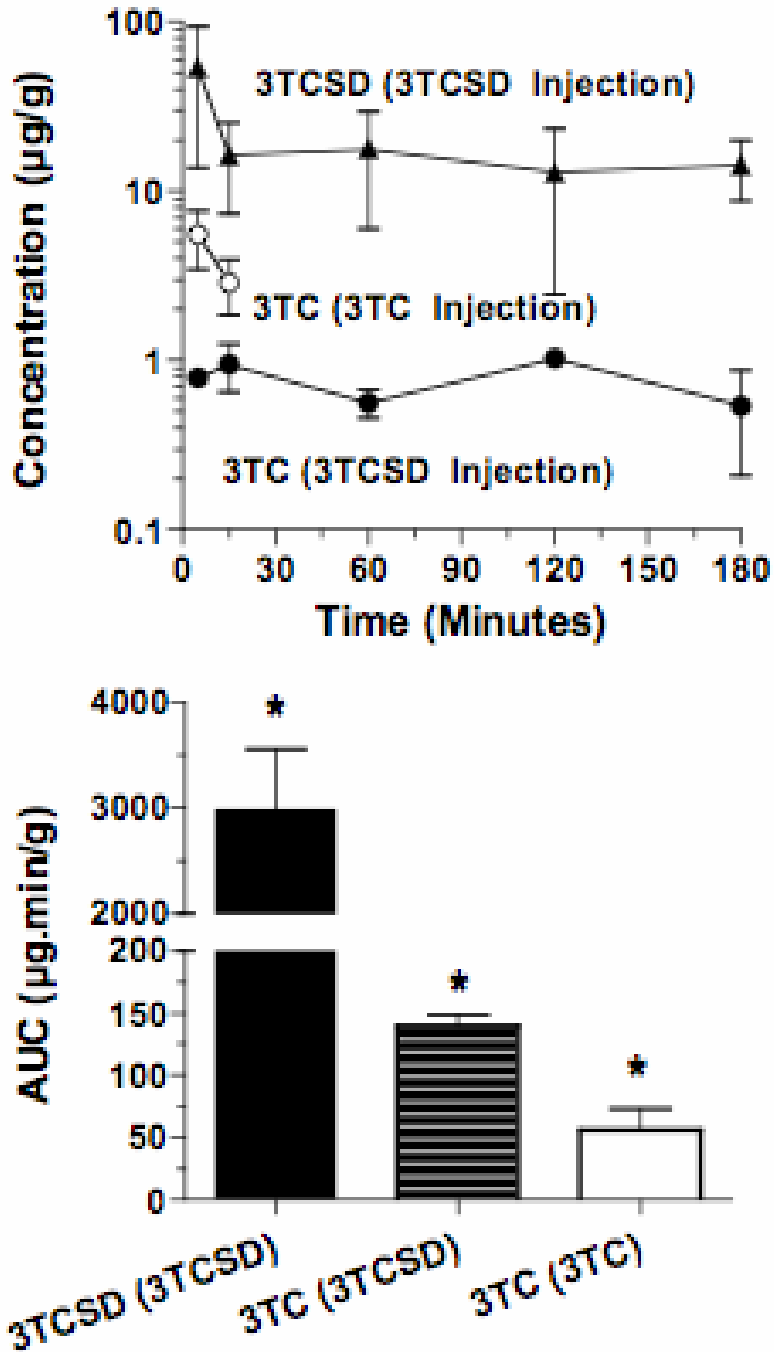


Figure 8: Liver concentration-time courses (top) and AUC values (bottom) of parent (3TC) and/or conjugated (3TCSD) lamivudine after iv administration of single, 5-mg/kg doses (3TC equivalent) of 3TC or 3TCSD to rats. Standard deviation values are shown as error bars (n = 3 rats for each time point). Asterisks indicate significant differences from the other two groups.

The kidney concentration-time courses (top) and AUC values (bottom) of the conjugate and regenerated 3TC after the administration of the conjugate and those of 3TC after the injection of the parent drug itself are depicted in Fig. 9. In addition to the liver (Fig. 8), kidney was the only other organ where high concentrations of the conjugated and regenerated 3TC were found (Fig. 9). In contrast to the liver (Fig. 8), however, relatively high and persistent concentrations of 3TC were found in the kidney even after the injection of the parent drug (Fig. 9).

In contrast to the liver (Fig. 8) and kidneys (Fig. 9), the concentrations of the conjugate and/or regenerated 3TC were very low or undetectable in the lungs, spleen, and heart after 3TCSD injection (data not shown). Additionally, no released 3TC could be detected in these tissues. The concentrations of 3TC after 3TC injection in organs other than kidney were also low or below the limit of detection in most of the samples.

Table 7 shows the AUC ratio of regenerated 3TC after 3TCSD injection over 3TC after 3TC injection for all the studied tissues. The ratio is highest for the liver, while it is zero for tissues like spleen, heart, and lung. For

the kidney, the ratio is less than 1 (Table 7).

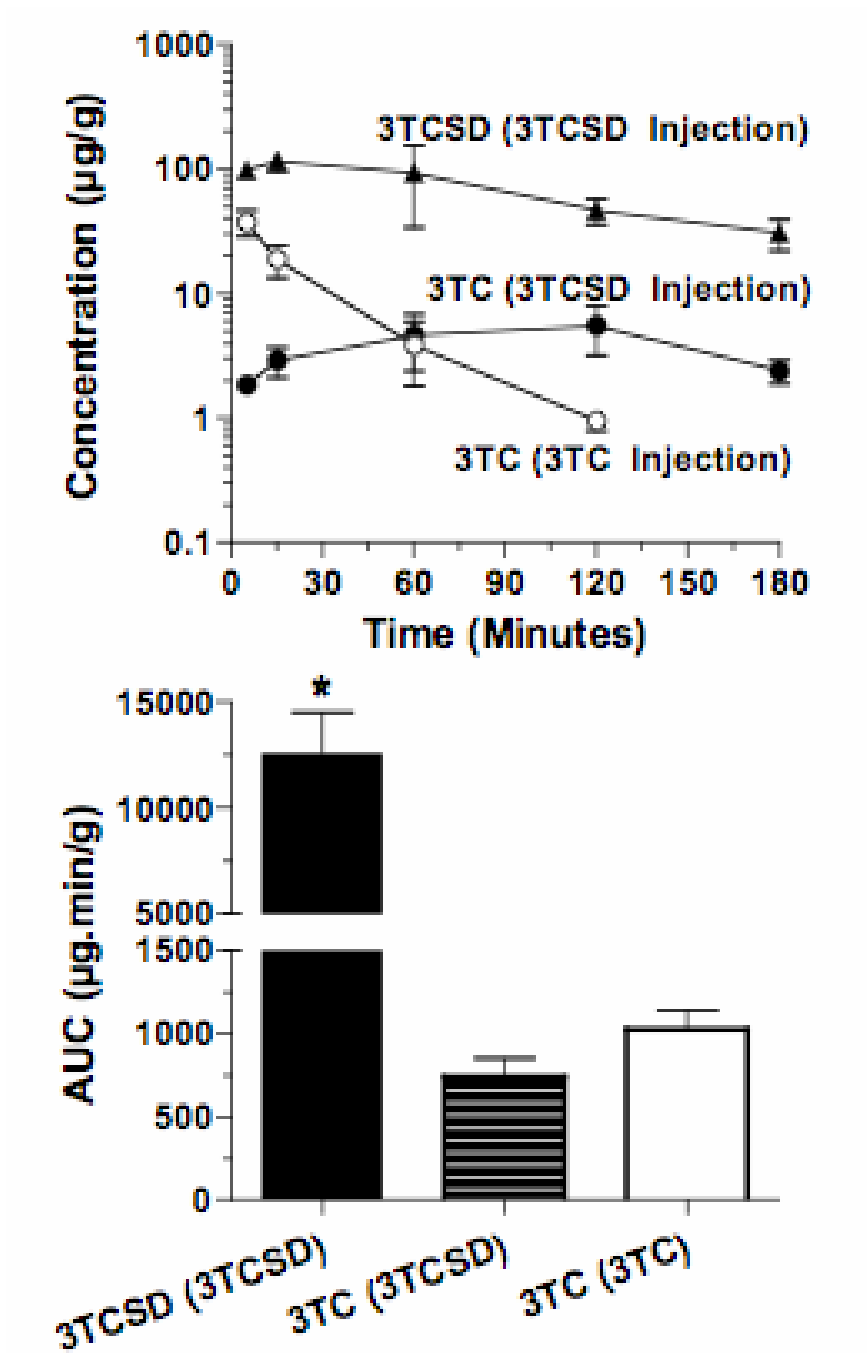


Figure 9: Kidney concentration-time courses (top) and AUC values (bottom) of parent (3TC) and/or conjugated (3TCSD) lamivudine after iv administration of single, 5-mg/kg doses (3TC equivalent) of 3TC or 3TCSD to rats. Standard

deviation values are shown as error bars (n = 3 rats for each time point). Asterisk indicates significant differences from the other two groups.

Table 7 : Ratios of the regenerated 3TC AUC after 3TCSD over parent 3TC AUC after 3TC in all the studied tissues after iv administration of single, 5-mg/kg doses (3TC equivalent) of 3TC or 3TCSD to rats.

Tissue	Regenerated 3TC/Parent 3TC AUC Ratio
Liver	2.41
Kidney	0.721
Spleen	0
Heart	0
Lung	0

CHAPTER IV

DISCUSSION

Targeted delivery of anti-HBV drugs to the liver, for the treatment of viral hepatic diseases, has attracted the attention of scientists for several years. In one of the first publications on this subject, Balboni et al. (Balboni et al., 1976) showed that conjugation of cytosine arabinoside and 5-fluorodeoxyuridine to albumin resulted in accumulation of these antiviral drugs in the mouse liver cells, increasing the effectiveness of the drugs in comparison with the free drugs. Further works by Fiume and colleagues (Fiume et al., 1997b) modified this strategy by the use of lactosaminated albumin as the carrier, selectively targeting the asialoglycoprotein receptors on the hepatocytes with the galactose moiety of lactose. Additionally, conjugates of antiviral drugs with galactosylated poly-L-lysine, instead of albumin, have been synthesized and tested by the same group (Fiume et al., 1986); (Fiume et al., 1997a). Others have used arabinogalactan (Enriquez et al., 1995) or glycosylated lipoproteins (Bijsterbosch et al., 1996, [de Vrueth, 2000 #355]) as liver-accumulating carriers, or prodrugs that release the active drug based on metabolism by hepatic cytochrome P450 (Erion et al., 2005); (Reddy et al., 2005) for targeted delivery of antiviral drugs to the liver. These studies support the general concept that targeted delivery of antiviral drugs to the liver potentially increases the efficacy of these drugs in the treatment of viral liver infections while, at the same time, decreasing their toxic effects in other tissues. However, the choice of carrier and

